# *Borrelia burgdorferi* PlzA is a cyclic-di-GMP dependent DNA- and RNA-binding protein

Nerina Jusufovic[1], Andrew C. Krusenstjerna[1], Christina R. Savage[1], Timothy C. Saylor[1], Catherine A. Brissette[2], Wolfram R. Zückert[3], Paula J. Schlax[4], Md A. Motaleb[5], and Brian Stevenson[1,6,*]

[1] Microbiology, Immunology and Molecular Genetics, University of Kentucky College of Medicine, University of Kentucky, Lexington, Kentucky, 40526-0001, USA [2] Department of Biomedical Sciences, University of North Dakota, School of Medicine and Health Sciences, Grand Forks, ND 58203-9061, USA, [3] Department of Microbiology, Molecular Genetics and Immunology, University of Kansas School of Medicine, Kansas City, KS 66160, USA, [4] Department of Chemistry and Biochemistry, Bates College, Lewiston, ME, 04240-6030, USA, [5] Department of Microbiology and Immunology, Brody School of Medicine, East Carolina University, Greenville, NC 27834-435, USA, and [6] Department of Entomology, University of Kentucky, Lexington, Kentucky, 40526-0001, USA.

* To whom correspondence should be addressed. Tel: +1 859 257 9358; Fax: 859 257 8994; Email: brian.stevenson@uky.edu

## ABSTRACT

The PilZ domain-containing protein, PlzA, is the only cyclic di-GMP binding protein encoded by all Lyme disease spirochetes. PlzA has been implicated in the regulation of many borrelial processes, but the effector mechanism of PlzA was not previously known. Here we report that PlzA can bind DNA and RNA, and that nucleic acid binding requires c-di-GMP. In studies with the promoter and 5' UTR of the glycerol catabolism operon, *glpFKD*, the affinity of PlzA for nucleic acids increased as concentrations of c-di-GMP were increased. A mutant PlzA that is incapable of binding c-di-GMP did not bind to any tested nucleic acids. PlzA is a dual-domain protein consisting of a PilZ-like N-terminal domain linked to a canonical C-terminal PilZ domain. Dissection of the domains demonstrated that the separated N-terminal domain bound nucleic acids independently of c-di-GMP. The C-terminal domain, which includes the c-di-GMP binding motifs, did not bind nucleic acids under any tested conditions. Our data are supported by computational docking, which predicts that c-di-GMP binding at the C-terminal domain stabilizes the overall protein structure and facilitates PlzA-DNA interactions via residues in the N-terminal domain. Based on our data, we propose that levels of c-di-GMP during the various stages of the enzootic life cycle dictate PlzA regulatory targets and functions.

34 **INTRODUCTION**

35 Cyclic bis-(3'→5')-dimeric guanosine monophosphate (c-di-GMP), is a ubiquitous bacterial
36 cyclic di-nucleotide. In many bacterial species, it engages in the regulation of key processes
37 such as transcription, motility, biofilm formation, and virulence (Ryjenkov *et al.*, 2005; Hengge,
38 2009; Romling *et al.*, 2013; Jenal *et al.*, 2017; Valentini and Filloux, 2019). The Lyme disease
39 spirochete, *Borrelia burgdorferi* sensu lato, referred to as *Borrelia burgdorferi* henceforth, has
40 a c-di-GMP regulatory network consisting of a transmembrane sensor histidine kinase (Hk1),
41 a response regulator diguanylate cyclase (Rrp1), two phosphodiesterases (PdeA and PdeB),
42 and a single, chromosomally encoded PilZ domain-containing protein, PlzA (Galperin *et al.*,
43 2001; Freedman *et al.*, 2009; Rogers *et al.*, 2009; Sultan *et al.*, 2010; Caimano *et al.*, 2011;
44 Sultan *et al.*, 2011; Novak *et al.*, 2014).

45 The borrelial Hk1/Rrp1 two-component system synthesizes c-di-GMP; activation of Hk1
46 (BB_0420) occurs through an unknown signal (Caimano *et al.*, 2011; Bauer *et al.*, 2015). Rrp1
47 (BB_0419), the only identified diguanylate cyclase in *B. burgdorferi,* synthesizes c-di-GMP
48 from two GTP molecules and is essential for acquisition and survival in the tick vector (Rogers
49 *et al.*, 2009; Kostick *et al.*, 2011). Turnover of c-di-GMP is mediated by PdeA (BB_0363) and
50 PdeB (BB_0374), the only phosphodiesterases present in *B. burgdorferi*, which degrade c-di-
51 GMP to pGpG and GMP, respectively (Sultan *et al.*, 2010; Sultan *et al.*, 2011). *B. burgdorferi*
52 must delicately balance c-di-GMP signaling, as c-di-GMP is required for both maintenance in
53 the tick vector and successful transmission into the vertebrate host, but constitutive synthesis
54 is detrimental to spirochete survival during vertebrate infection (Sultan *et al.*, 2010; Sultan *et*
55 *al.*, 2011; Caimano *et al.*, 2015; Groshong *et al.*, 2021).

56 Synthesized c-di-GMP is bound by PlzA, the only universal c-di-GMP binding protein found in
57 all isolates of Lyme disease *Borreliae* (Kostick-Dunn *et al.*, 2018). Mutation of *plzA* has been
58 implicated in many *B. burgdorferi* phenotypes, including mis-regulation of alternative
59 carbohydrate utilization, decreased motility, and virulence defects (Pitzer *et al.*, 2011; He *et*
60 *al.*, 2014; Mallory *et al.*, 2016; Zhang *et al.*, 2018; Groshong *et al.*, 2021). Binding of c-di-GMP

61 induces conformational changes in PlzA structure, which has led to the hypothesis that c-di-
62 GMP binding acts as a switching mechanism providing the holo and apo-forms of PlzA with
63 distinct functions (Mallory *et al.*, 2016; Groshong *et al.*, 2021; Grassmann *et al.*, 2023).
64 Specifically, c-di-GMP bound PlzA is thought to regulate genes required for survival in the tick
65 host, while apo-PlzA is speculated to play a role in regulation during vertebrate infection
66 (Groshong *et al.*, 2021; Grassmann *et al.*, 2023).

67 A common mechanism of action for c-di-GMP effector proteins is to bind nucleic acids (Wilksch
68 *et al.*, 2011; Tschowri *et al.*, 2014; Tan *et al.*, 2015; Wang *et al.*, 2016; Schäper *et al.*, 2017;
69 Hsieh *et al.*, 2018; Skotnicka *et al.*, 2020). It has been hypothesized that PlzA could bind DNA
70 and regulate genes through impacts on transcription, such as directly interacting with RNA
71 polymerase (RNAP), but this has yet to be experimentally tested (Groshong *et al.*, 2021;
72 Grassmann *et al.*, 2023). Conversely, others have hypothesized that PlzA cannot bind DNA,
73 as it does not contain an obvious, conventional DNA binding motif (Caimano *et al.*, 2015;
74 Zhang *et al.*, 2018). Indeed, Zhang *et al.* concluded that PlzA does not bind DNA, as their
75 electrophoretic mobility shift assays (EMSA) did not identify binding (Zhang *et al.*, 2018). The
76 results and methodologies including protein and c-di-GMP concentrations, were not shown in
77 that report. After the submission of a preprint of our manuscript, another group published that
78 PlzA has RNA chaperone activity that is independent of c-di-GMP, supporting the notion that
79 holo- and apo-forms of PlzA have distinct functions (Van Gundy *et al.*, 2023).

80 Given the multiple, conflicting hypotheses regarding PlzA function, as well as the potential for
81 additional mechanisms between liganded and unliganded PlzA, we sought to further
82 characterize PlzA nucleic acid binding function. We decided to examine a known regulatory
83 target of PlzA, *glpFKD*, the glycerol catabolism operon. The *glpFKD* operon promotes *B.*
84 *burgdorferi* survival in ticks (Pappas *et al.*, 2011; Corona and Schwartz, 2015; Helble *et al.*,
85 2021). After a tick has completed the digestion of its blood meal, it is hypothesized that the
86 midgut is devoid of glucose and many other nutrients. To survive in that environment, Lyme
87 disease spirochetes would need to utilize alternate carbon sources such as glycerol, which is

88 available in the tick host (Lee and Baust, 1987). The *glpFKD* operon is regulated through the
89 Hk1/Rrp1 pathway, and borrelial *plzA* mutants are defective in glycerol metabolism (Rogers
90 *et al.*, 2009; He *et al.*, 2011; Caimano *et al.*, 2015; Zhang *et al.*, 2018). Further, PlzA was found
91 to both positively and negatively affect the *glp* operon, at higher and lower c-di-GMP levels,
92 respectively (Zhang *et al.*, 2018).

93 PlzA is classified as an xPilZ-PilZ domain protein given its dual-domain structure. The binding
94 of c-di-GMP to the interdomain linker and C-terminal PilZ domain results in a conformational
95 change; locking the C-terminal PilZ and N-terminal xPilZ domains into rigid conformation,
96 which we hypothesized could permit DNA binding (Mallory *et al.*, 2016; Groshong *et al.*, 2021;
97 Singh *et al.*, 2021). While no canonical DNA binding domain is evident in the PlzA amino acid
98 sequence, our lab has discovered and characterized multiple nucleic acid binding proteins
99 possessing novel binding motifs (Babb *et al.*, 2006; Riley *et al.*, 2009; Jutras *et al.*, 2012;
100 Jutras *et al.*, 2013a; Jutras *et al.*, 2013b; Zhang *et al.*, 2018; Singh *et al.*, 2021). Here, we
101 report that PlzA can bind DNA and RNA directly downstream of the promoter and into the 5'
102 untranslated region (UTR) of the *glpFKD* operon and that binding to this region is c-di-GMP
103 dependent.

104 **RESULTS**

105 **PlzA binds *glpFKD* DNA and the interaction is c-di-GMP dependent**

106 Previous studies demonstrated that c-di-GMP and PlzA modulate expression of the glycerol
107 metabolism operon (Rogers *et al.*, 2009; He *et al.*, 2011; Caimano *et al.*, 2015; Zhang *et al.*,
108 2018). Activation of *glpFKD* is critical for spirochete survival in between blood meals of the tick
109 vector, which requires catabolism of glycerol (He *et al.*, 2011; Pappas *et al.*, 2011; Zhang *et*
110 *al.*, 2018). Given that requirement, we hypothesized that PlzA might bind 5' of the *glpFKD*
111 operon. To that end, we sought to determine if PlzA could bind DNA between *glpFKD* and the
112 upstream ORF BB_0239, which encodes a deoxyguanosine/deoxyadenosine kinase. The
113 transcriptional boundaries and promoter elements of the *glpFKD* operon were previously

114 mapped (Adams *et al.*, 2017; Grove *et al.*, 2017). A fluorescently labeled DNA fragment was
115 generated by PCR amplification from a plasmid containing the 410 bp intergenic region
116 between the upstream gene, and the start of *glpF* (BB_0240) and is denoted as *glpFKD*(-219)
117 (Figure 1).

118 To assess if PlzA could bind this region of DNA, EMSAs with increasing concentrations of
119 recombinant PlzA were performed (Figure 2A). Binding was observed at higher micromolar
120 concentrations, as evidenced by the disappearance of free DNA. The experiment was
121 repeated with added non-specific competitor poly-dI-dC to a final concentration of 2.5 ng/μL.
122 Poly-dI-dC did not appreciably compete away the shifted protein-DNA complexes (Figure 2B).

123 Given that binding of c-di-GMP has been hypothesized to act as a switching mechanism for
124 PlzA function, we next assessed the effects of c-di-GMP on DNA binding. EMSA reaction
125 mixtures were supplemented with exogenous c-di-GMP to a final concentration of 100 μM.
126 This concentration was used to saturate all PlzA molecules present in the reaction to ensure
127 complete binding throughout electrophoresis. Saturating concentrations have similarly been
128 used in other studies with c-di-GMP binding proteins that also bind DNA (Wilksch *et al.*, 2011;
129 Yang *et al.*, 2013; Tan *et al.*, 2015; Zamorano-Sánchez *et al.*, 2015; Schäper *et al.*, 2017;
130 Skotnicka *et al.*, 2020). The EMSA with *glpFKD*(-219), poly-dI-dC, and increasing PlzA was
131 repeated with the supplemented c-di-GMP (Figure 2C). The addition of c-di-GMP enhanced
132 PlzA binding affinity for *glpFKD*(-219), resulting in binding at lower concentrations of protein,
133 and the formation of distinct protein-DNA complexes as indicated by the arrows. Further, as
134 PlzA concentration increased, the mobility of the shifted band decreased.

135 To further assess the requirement of c-di-GMP for PlzA DNA binding activity, a double mutant
136 PlzA protein ($PlzA_{RD\text{-}RD}$) that cannot bind c-di-GMP was produced by site-directed
137 mutagenesis which replaced key arginine residues in the conserved c-di-GMP binding motif,
138 RxxxR, with aspartic acids (Ryjenkov *et al.*, 2006; Amikam and Galperin, 2006; Chou and
139 Galperin, 2016). These mutations resulted in the amino-acid substitutions R145D and R149D

140 within the c-di-GMP binding site of PlzA and have previously been shown to abolish c-di-GMP
141 binding (Freedman *et al.*, 2009; Mallory *et al.*, 2016; Singh *et al.*, 2021). The *glpFKD*(-219)
142 EMSAs were repeated with $PlzA_{RD-RD}$ (Figure 2D-F). Binding to *glpFKD*(-219) was not
143 observed under any tested conditions with $PlzA_{RD-RD}$.

144 To ensure binding was not due to recognition of vector derived sequences within the probe,
145 competition EMSAs were performed with unlabeled DNA competitors derived from empty pCR
146 2.1 TA clones, or those containing the *glpFKD*(-219) sequence (Figure 3A). The nonspecific
147 DNA from the empty pCR 2.1 vector did not compete away $PlzA_{WT}$-*glpFKD*(-219) complexes
148 at a 20-fold higher concentration (Figure 3B, lanes 3-5). Meanwhile, as little as 6-fold molar
149 excess of unlabeled *glpFKD*(-219) was able to compete with the probe, and a 10-fold molar
150 excess successfully competed away the $PlzA_{WT}$-*glpFKD*(-219) complexes (Figure 3B, lanes
151 6-8). These results demonstrate PlzA preferentially bound the *glpFKD*-derived sequences.

152 Noting that c-di-GMP enhanced DNA binding by PlzA yet free DNA decreased with purified
153 recombinant PlzA without adding exogenous c-di-GMP, we investigated the possibility that
154 PlzA was being purified with c-di-GMP already bound. Purified recombinant proteins were
155 prepared and assayed by liquid chromatography-tandem mass spectrometry. Extracted ion
156 chromatograms showed the presence of c-di-GMP in $PlzA_{WT}$ protein preparations but not in
157 $PlzA_{RD-RD}$ preparations (Figure 4). The concentration of c-di-GMP present in recombinant
158 $PlzA_{WT}$ was extrapolated from a c-di-GMP standard curve at 99.29 nM. A total of 31.7 μM of
159 protein had been analyzed, indicating that approximately 0.3% of the protein was bound with
160 c-di-GMP. Prior studies have reported dissociation constants of 1.25 to 6.25 μM of PlzA for c-
161 di-GMP, which are typical $K_D$ values for PilZ receptors and c-di-GMP (Pitzer *et al.*, 2011;
162 Mallory *et al.*, 2016). The amount of co-purified c-di-GMP detected is lower than the $K_D$. This
163 is likely due to removal of some c-di-GMP during the protein purification process, as well as
164 *E. coli* maintaining low cellular concentrations of c-di-GMP (~40-80 nM) (Sarenko *et al.*, 2017;
165 Junkermeier and Hengge, 2023). Taken together, these data indicate that PlzA DNA binding
166 to this region of the *glpFKD* operon is specific and c-di-GMP dependent.

167 **c-di-GMP levels modulate PlzA DNA binding affinity**

168 It was previously identified with *glpFKD-gfp* promoter fusion studies that the minimal *glpFKD*
169 promoter sequence (-46 relative to the *glpFKD* transcription start site) with the full 195bp UTR
170 region was expressed at higher levels than the core promoter sequence alone (Grove *et al.*,
171 2017). Given these findings and our data that PlzA can bind DNA, we focused further analysis
172 of PlzA binding on a smaller sequence within that region that was found to be important for
173 transcription (Grove *et al.*, 2017; Savage *et al.*, 2018). A 42 bp DNA probe encompassing the
174 -7 to +35 sites, called *glpFKD*(-7/+35), was generated by annealing complementary
175 oligonucleotides with the forward oligonucleotide 5' conjugated to IRDye800 (Figure 5A). An
176 RNA probe conjugated to Alexa Fluor 488 was also made for subsequent RNA binding studies.

177 To determine how different c-di-GMP levels impact PlzA binding affinity, EMSAs with
178 increasing $PlzA_{WT}$ concentrations were performed at concentrations of added c-di-GMP
179 ranging from 0 to 100 μM in the reaction mixtures with the *glpFKD*(-7/+35) probe (Figure 5B).
180 Competitor poly-dI-dC was added at a final concentration of 2.5 ng/μL to reduce nonspecific
181 interactions. $PlzA_{WT}$ bound to *glpFKD*(-7/+35), and binding was enhanced by increasing the
182 concentration of c-di-GMP. In reactions with no added c-di-GMP, we observed that the amount
183 of free DNA decreased with increasing PlzA concentrations but did not detect a band
184 corresponding to the protein-DNA complex. The decrease in free DNA with no added c-di-
185 GMP is presumably due to the presence of co-purified c-di-GMP in recombinant PlzA. When
186 equimolar c-di-GMP and protein levels were tested, a discernable shift (formation of a new
187 band) was evident only at protein concentrations greater than 2.5 μM (purple arrow). As c-di-
188 GMP concentrations were further increased, shifts became discernable at lower protein
189 concentrations, with the strongest binding observed at c-di-GMP concentrations of 25, 50, and
190 100 μM. Further, as protein concentration was increased, we consistently observed
191 progressive super-shifting of complexes in a dose-dependent manner (Figure 5B, colored
192 arrows). At protein concentrations greater than or equal to 5 μM coupled with c-di-GMP
193 concentrations greater than 25 μM, complexes appeared to smear, suggesting the observed

194 super-shifting is due to complex dissociation. The stoichiometry of this complex(es) is under
195 investigation.

196 Next, we calculated the apparent binding affinity ($K_{D(app)}$) under these experimental conditions
197 for PlzA for *glpFKD*(-7/+35) at the various c-di-GMP concentrations (Figure 5C). The
198 calculations were performed under the assumption that a single molecule of PlzA binds to a
199 single molecule of DNA. As noted above, it is possible that the protein-nucleic acid ratio is not
200 1:1, which could affect the calculated values. The values described below are the $K_{D(app)}$ ±
201 SEM (standard error of the mean). Without any supplemented c-di-GMP, the extrapolated
202 $K_{D(app)}$ of $PlzA_{WT}$-*glpFKD*(-7/+35) was calculated as 7.86 (± 1.84 μM), however we again note
203 that some c-di-GMP is already present in the $PlzA_{WT}$ protein preparations (see above and
204 Figure 4). Binding affinity increased approximately 1.5-fold under equimolar c-di-GMP and
205 protein concentrations with a calculated $K_{D(app)}$ of 4.22 (± 0.43 μM). Under saturating c-di-GMP
206 conditions (exceeding the $K_D$ of PlzA for c-di-GMP), binding affinity increased further.
207 Supplementing binding reactions with 10 μM c-di-GMP improved PlzA-DNA binding 2.5-fold
208 ($K_{D(app)}$ of 2.81 (± 0.50 μM). An approximately 6- to 7-fold increase in binding affinity was
209 observed when the binding reaction was supplemented with either 25, 50, or 100 μM of c-di-
210 GMP resulting in calculated $K_{D(app)s}$ of 1.33 (± 0.12 μM), 1.25 (± 0.08 μM), and 1.09 μM (± 0.06
211 μM), respectively.

212 To determine if the calculated $K_{D(app)}$ values differed significantly, Welch's ANOVA followed by
213 a Dunnett's T3 multiple comparisons test was performed (Figure 5D). All calculated $K_{D(app)}$
214 values differed significantly ($p \leq 0.05$) from the 0 μM c-di-GMP $K_{D(app)}$ except for the equimolar
215 and 10 μM c-di-GMP conditions. Compared to the equimolar condition, the 25, 50, and 100
216 μM $K_{D(app)}$ values differed significantly ($p \leq 0.001$), while the 10 μM c-di-GMP $K_{D(app)}$ value did
217 not ($p > 0.05$). When comparing the 10, 25, 50, and 100 μM $K_{D(app)}$ values of $PlzA_{WT}$-*glpFKD*(-
218 7/+35) interaction, there were no significant differences ($p > 0.05$). The mutant $PlzA_{RD\text{-}RD}$ did
219 not bind *glpFKD*(-7/+35) under any tested conditions (Figure 5E). Overall, we conclude that
220 levels of c-di-GMP significantly impact PlzA-DNA binding.

221 **PlzA also binds *glp*-derived single-stranded nucleic acids**

222 Several borrelial proteins that were initially identified as having affinities for DNA have
223 subsequently been found to also bind RNA (Jutras *et al.*, 2013a; Savage *et al.*, 2018;
224 Krusenstjerna *et al.*, 2023). Given the role the 5' UTR of the *glpFKD* operon plays in its
225 regulation, we hypothesized PlzA could potentially also bind RNA. RNA probes used were
226 designed to correspond to only transcribed regions (Figure 5A). The *glpFKD*(-7/+35)
227 counterpart RNA probe is designated *glpFKD*(UTR). EMSAs were performed with increasing
228 concentrations of $PlzA_{WT}$ with 0 μM, 100 μM, or equimolar c-di-GMP levels and labeled
229 *glpFKD*(UTR) (Figure 6A). We did not test additional c-di-GMP concentrations that were tested
230 for impacts on DNA binding for the RNA, as no significant difference was found between 100
231 μM c-di-GMP and the other tested c-di-GMP concentrations. $PlzA_{WT}$ bound the RNA, which
232 was enhanced by addition of c-di-GMP (Figure 6A). The binding pattern to the *glpFKD*(UTR)
233 RNA was comparable to the *glpFKD*(-7/+35) DNA, with increased protein and c-di-GMP
234 concentrations leading to an increase in the size of the PlzA-RNA shifts.

235 EMSAs were repeated with the $PlzA_{RD\text{-}RD}$ mutant protein at 0 or 100 μM c-di-GMP (Figure 6B).
236 The $PlzA_{RD\text{-}RD}$ protein did not bind *glpFKD*(UTR) RNA at any tested protein concentration,
237 regardless of whether c-di-GMP was included.

238 Given that PlzA can bind to both the DNA and RNA, we sought to determine if it could also
239 bind the cognate ssDNA corresponding to the coding strand. This is relevant as ssDNA is
240 exposed at open transcriptional complexes. The forward, IRDye labeled oligonucleotide used
241 to generate the *glpFKD*(+7/-35) dsDNA probe was used as a single-stranded DNA probe
242 (ss*glpF*) in EMSAs. No evident complexes were formed when exogenous c-di-GMP was
243 excluded from EMSA reactions, but free ssDNA did decrease at the highest tested PlzA
244 concentrations of 3.5-7.5 μM (Figure 6C right panel). Adding 100 μM c-di-GMP resulted in the
245 formation of PlzA-ssDNA complexes but at higher concentrations of protein than required to
246 achieve complex formation with dsDNA and RNA (Figure 6C left panel).

247 We next quantified the binding affinity of PlzA for the *glp* derived RNA and ssDNA sequences
248 through densitometry of the EMSA shifts, and the apparent $K_{D(app)s}$ calculated as described
249 above (Figure 6D). As with dsDNA, the binding affinity of PlzA for RNA was weakest when no
250 exogenous c-di-GMP was supplemented with a calculated $K_{D(app)}$ of 7.64 (± 1.85 μM). Binding
251 improved approximately 2-fold in equimolar c-di-GMP conditions with a $K_{D(app)}$ of 4.14 (± 0.74
252 μM). The $K_{D(app)}$ was 0.95 (± 0.11 μM) when the c-di-GMP concentration was 100 μM, an 8-
253 fold increase in PlzA binding affinity for the *glpFKD*(UTR) RNA as compared to when no c-di-
254 GMP was added. There was a significant difference between the $PlzA_{WT}$-*glpFKD*(UTR) RNA
255 $K_{D(app)}$ value calculated at 100 μM c-di-GMP and both the equimolar and 0 μM c-di-GMP values
256 ($p \leq 0.01$) (Figure 7A). No significant differences were detected between the $K_{D(app)}$ values
257 calculated at 0 μM and equimolar c-di-GMP levels ($p > 0.05$).

258 Although PlzA bound the ss*glpF* probe, it had a substantially lower affinity for ssDNA than
259 dsDNA or RNA (Figure 6D). The $K_{D(app)}$ of the $PlzA_{WT}$-ss*glpF* interaction was 8.74 (± 1.86 μM)
260 with 0 μM c-di-GMP and 4.42 (± 0.90 μM) with 100 μM c-di-GMP. These values were found to
261 be statistically significant from one another ($p < 0.05$) (Figure 7B). Only a 2-fold increase in
262 binding affinity of PlzA for the single-strand DNA was observed when the c-di-GMP
263 concentration was increased to 100 μM, whereas the same concentration of c-di-GMP
264 increased PlzA binding affinity 7-fold for dsDNA and 8-fold for RNA.

265 Lastly, we also compared the binding affinities of PlzA for all three tested nucleic acids (Figure
266 7C). The calculated $K_{D(app)}$ values of $PlzA_{WT}$ for each nucleic acid in the presence of 100 μM
267 c-di-GMP were compared with a Welch's ANOVA and Dunnett's T3 multiple comparisons test.
268 No significant difference ($p > 0.05$) was detected between the PlzA $K_{D(app)}$ values for dsDNA
269 (1.09 ± 0.06 μM) and RNA (0.95 ± 0.11 μM), indicating that PlzA binds the *glpFKD* dsDNA
270 and RNA with similar affinity. Both the dsDNA and RNA $K_{D(app)s}$ were significantly different from
271 the calculated ssDNA $K_{D(app)}$ (4.42 ± 0.90 μM) ($p \leq 0.01$), suggesting that PlzA prefers *glp*-
272 derived dsDNA and RNA over ssDNA. All the binding data presented throughout the

273 manuscript are summarized in Table 1. Collectively, our data indicate that PlzA binding activity
274 is c-di-GMP dependent for all tested *glpFKD* nucleic acids.

275 **Dissection of PlzA reveals the nucleic acid binding domain**

276 The first discovered c-di-GMP binding receptors were the PilZ domain-containing proteins
277 (Ryjenkov *et al.*, 2006; Amikam and Galperin, 2006; Galperin and Chou, 2020). The PilZ
278 domain consists of two conserved c-di-GMP binding motifs, RxxxR and [D/N]ZSXXG
279 (Ryjenkov *et al.*, 2006; Amikam and Galperin, 2006; Chou and Galperin, 2016; Cheang *et al.*,
280 2019). The recently solved crystal structure of *B. burgdorferi* PlzA revealed a unique dual-
281 domain topology consisting of an amino-terminal PilZ-like domain, called PilZN3, which is
282 connected to the carboxy-terminal PilZ domain via a linker domain that contains the RxxxR c-
283 di-GMP binding motif (Singh *et al.*, 2021). The first 141 amino acid residues make up the N-
284 terminus of PlzA ($PlzA_{NTD}$), while residues 142-261 make up the C-terminal ($PlzA_{CTD}$) PilZ
285 domain. Having determined that PlzA is a c-di-GMP-dependent DNA and RNA binding protein,
286 we next sought to determine which domain of PlzA binds nucleic acid. To generate
287 recombinant $PlzA_{NTD}$ and $PlzA_{CTD}$ domains, truncated *plzA* genes called *plzA*-NTD and *plzA*-
288 CTD were cloned to encode the residues described above, which correspond to each
289 respective domain (Figure 8A).

290 EMSAs were performed with labeled *glpFKD*(-7/+35) DNA probe and increasing
291 concentrations of $PlzA_{NTD}$ or $PlzA_{CTD,}$ with or without 100 μM c-di-GMP. $PlzA_{NTD}$ bound DNA
292 independently of c-di-GMP, as supplementation with c-di-GMP did not affect binding (Figure
293 8B). $PlzA_{CTD}$ contains the motifs required for c-di-GMP binding, but the $PlzA_{CTD}$ domain did not
294 bind to DNA with or without added c-di-GMP (Figure 8C). It was also determined that $PlzA_{NTD}$
295 could bind *glpFKD*(UTR) RNA with or without c-di-GMP, while $PlzA_{CTD}$ does not (Figure 8D
296 and E respectively).

297 We also performed the LC/MS-MS analysis on $PlzA_{NTD}$ and $PlzA_{CTD}$ recombinant proteins to
298 determine if any di-nucleotides were present (Figure 9A). Co-purified c-di-GMP was detected

299 in $PlzA_{CTD}$ but not $PlzA_{NTD}$ by LC/MS-MS. The concentration of c-di-GMP present in
300 recombinant $PlzA_{CTD}$ was determined as 704.29 nM. A total of 66.7 μM of protein was sent for
301 analysis indicating approximately 1.1 % of $PlzA_{CTD}$ was bound with c-di-GMP. This indicates
302 that $PlzA_{CTD}$ retained the ability to bind c-di-GMP but cannot bind nucleic acid.

303 To confirm that the truncated proteins were stable, circular dichroism (CD) was performed,
304 and the CD spectra were obtained for $PlzA_{WT}$, $PlzA_{RD\text{-}RD}$, $PlzA_{NTD}$, and $PlzA_{CTD}$ in the binding
305 buffer used for EMSAs (Figure 9B). The CD results show that the mutated proteins retained
306 stable structures matching that of $PlzA_{WT}$. Therefore, the lack of DNA binding by $PlzA_{RD\text{-}RD}$ and
307 $PlzA_{CTD}$ is not due to improper folding.

308 **Computational docking of PlzA-nucleic acid interactions**

309 To gain a better understanding of the interactions between PlzA and DNA or RNA, we
310 performed a computational docking analysis with the HDOCK server (Huang and Zou, 2014;
311 Yan *et al.*, 2017a; Yan *et al.*, 2017b; Yan *et al.*, 2020). The *glpFKD*(-7/+35) DNA and
312 *glpFKD*(UTR) RNA sequences were input as ligands, while the PlzA crystal structure (PDB
313 ID: 7mie) was input as the receptor molecule. The modeling results indicate that interactions
314 between PlzA and *glpFKD*(-7/+35) DNA are facilitated primarily through the N-terminal domain
315 (Figure 10a). Beta-strands six and seven of the N-terminus are extended and protrude
316 outward, intercalating a major groove of the DNA 5' to the protein docking site (Figure 10a top
317 panel). Polar and positively charged amino acids, including N110 and K111, are located at the
318 loop region where beta-strands 6 and 7 converge, with the potential to directly interact with
319 bases of the DNA (Rooman *et al.*, 2002; Sathyapriya and Vishveshwara, 2004). Interactions
320 with a minor groove of the DNA are predicted to occur through the loop region of beta-strands
321 2 and 3 and an unstructured linker region (Figure 10a bottom panel). Several positively
322 charged residues, including arginine (R32 and R38) and lysine (K81), as well as an aromatic
323 phenylalanine residue (F45), are predicted to directly interact with the minor groove and
324 backbone of the DNA. An additional lysine residue K87 located in the unstructured region,

325 protrudes and interacts directly with bases of another major groove of *glpFKD*(-7/+35). No
326 residues of the C-terminal domain are predicted to interact directly with the DNA; however,
327 four residues are interfacing the DNA (K161, I213, D258, and N261). Residue K161 hovers
328 over the DNA backbone potentially interacting nonspecifically via electrostatic interactions.
329 The computational docking data supports our EMSA data showing that $PlzA_{NTD}$ binds DNA
330 while $PlzA_{CTD}$ does not (Figures 8B and C).

331 The docking analysis was also performed with $PlzA_{WT}$ and *glpFKD*(UTR) RNA (Figure10B).
332 Again, the N-terminal domain of PlzA facilitates most of the interactions. Similar regions of the
333 protein that interacted with dsDNA are implicated in the interaction with RNA including the
334 residues of the loop region of beta-strands 6 and 7 (K111 and Y113), the loop region of beta-
335 strands 2 and 3 (R38, Y42, and F45) and the unstructured linker region (R32, D85, K87, F92,
336 and F95). Unlike the docking model with dsDNA, the PlzA-RNA docking model indicates more
337 involvement of the C-terminal domain in RNA binding. Several residues of alpha-helixes 5
338 (D155, R158, K159, and K161) and 6 (D258 and Y259) in the C-terminal domain of PlzA, are
339 predicted to interact with RNA. Although our EMSA results show that $PlzA_{CTD}$ does not bind
340 any tested nucleic acids, the docking results indicate it could help stabilize $PlzA_{NTD}$-nucleic
341 acid interactions or could be involved in target recognition. Several PlzA residues predicted to
342 be involved in nucleic-acid binding are currently being investigated by our lab.

343 Computational docking was attempted with PlzA and ss*glpF*, but the HDOCK server could not
344 complete the analysis. Given that PlzA bound dsDNA and RNA better than ssDNA, it is
345 interesting to note that the computational modeling predicts the RNA to fold into a double
346 stranded secondary structure. Combined with our EMSA data, this suggests that PlzA could
347 have a preference towards double stranded nucleic acids and/or secondary structures.

348 **DISCUSSION**

349 Cyclic-di-GMP has wide-ranging effects on many bacterial processes. The responses to c-di-
350 GMP are commonly mediated through c-di-GMP binding effector proteins. PlzA is the only

351 chromosomally and universally encoded c-di-GMP binding protein of the Lyme disease
352 spirochetes. It has been shown to be crucial for borrelial infection processes and in the
353 regulation of the metabolism of alternative carbon sources during colonization of vector ticks
354 (Pappas *et al.*, 2011; Pitzer *et al.*, 2011; He *et al.*, 2014; Mallory *et al.*, 2016; Zhang *et al.*,
355 2018; Groshong *et al.*, 2021). Despite its singularity and importance to *B. burgdorferi*, little was
356 previously known about the biochemical functions of PlzA outside of binding c-di-GMP. Here,
357 we provide evidence that PlzA is a novel c-di-GMP-dependent nucleic acid-binding protein.

358 While PlzA lacks an obvious canonical DNA binding motif, we hypothesized that PlzA might
359 be a nucleic acid binding protein given its role in the regulation of the *glpFKD* operon. Binding
360 was only observed by the wild-type PlzA protein but not the mutant, $PlzA_{RD\text{-}RD}$, which is
361 incapable of binding c-di-GMP. It has previously been shown that structural rearrangements
362 are induced upon the binding of c-di-GMP to PlzA (Mallory *et al.*, 2016; Groshong *et al.*, 2021).
363 Without bound c-di-GMP, PlzA has a structure that is flexible, potentially preventing the
364 interactions necessary for DNA binding. This hypothesis is supported by the fact that
365 crystallization of PlzA was only achieved with c-di-GMP bound (Singh *et al.*, 2021). We
366 surmise that binding of c-di-GMP to the C-terminal PilZ domain results in a conformational
367 change of PlzA into a more rigid structure permitting nucleic acid binding through residues of
368 the N-terminal domain.

369 We identified the N-terminal domain of PlzA as the nucleic acid binding domain and that
370 $PlzA_{NTD}$ bound DNA independently of c-di-GMP. In contrast, the C-terminal domain, $PlzA_{CTD}$,
371 did not bind any tested nucleic acids although it still bound c-di-GMP. While $PlzA_{NTD}$ can
372 interact with nucleic acids, these interactions are not as strong as $PlzA_{WT}$. Binding of nucleic
373 acid by $PlzA_{NTD}$ resulted in smeared shifts that lacked defined bands. This suggests instability
374 of the $PlzA_{NTD}$-nucleic acid complexes resulting in dissociation of the complexes during
375 electrophoresis. Noting that binding of c-di-GMP appears to stiffen interactions between the
376 N- and C-terminal domains, we hypothesize the C-terminal domain stabilizes the interactions
377 of $PlzA_{NTD}$ with nucleic acids when c-di-GMP bound. On the other hand, we posit that the

378 flexibility of apo-PlzA results in the C-terminal domain disrupting the ability of the N-terminal
379 domain to bind DNA. Although the N- and C- terminal PlzA domains are similar, structural
380 comparisons of $PlzA_{NTD}$ and $PlzA_{CTD}$ reveal distinct differences (Figure 8). The N-terminus of
381 $PlzA_{NTD}$ contains an alpha-helix that is absent in the N-terminus of $PlzA_{CTD}$. Additionally, an
382 alpha-helix is present at the beta-barrel pore of $PlzA_{NTD}$ but not in the $PlzA_{CTD}$. These
383 differences suggest distinct roles in PlzA-nucleic acid binding dynamics. We are currently
384 exploring the sequence motifs recognized by PlzA and the exact amino acid residues involved
385 in nucleic acid binding.

386 Previous studies found that PlzA is a monomer in solution regardless of c-di-GMP (Mallory *et*
387 *al.*, 2016). While many DNA-binding proteins bind DNA as dimers, alternative binding models
388 exist (Kim and Little, 1992; Kohler *et al.*, 1999). It has been shown that some proteins are
389 capable of binding sequentially as monomers which then multimerize on the DNA via protein-
390 protein interactions, such as some members of the Leucine zipper and helix-loop-helix zipper
391 families, the LexA repressor of *E. coli*, and BpaB of *B. burgdorferi* (Kim and Little, 1992; Kohler
392 *et al.*, 1999; Burns *et al.*, 2010). Our studies revealed that increasing c-di-GMP and $PlzA_{WT}$
393 concentrations resulted in progressively slower migration of PlzA-*glpFKD*(-7/+35) DNA
394 complexes. The decreases in the migration of the complexes that are observed with increasing
395 protein concentration may indicate a stoichiometry that is not 1:1, or the observed smearing
396 may be the result of dynamic equilibrium of the complexes in the gels during electrophoresis
397 (Fried and Crothers, 1981; Fried, 1989). While increasing c-di-GMP enhances PlzA binding,
398 there could be a threshold where too much c-di-GMP could be inhibitory and cause
399 dissociation of PlzA from nucleic acids. A dimerization or protein-protein interaction
400 residue/motif/domain remains to be identified in PlzA, and work is ongoing to address the
401 DNA-binding mode and stoichiometry of PlzA-nucleic acid complexes.

402 We also observed probe signal in the gel wells at high protein and c-di-GMP concentrations.
403 This could be due to protein aggregation. Rather than simply being a negative consequence
404 of environmental stress, recent studies indicate a role for protein aggregation in regulation.

405 Specifically, certain conditions can induce a protein to aggregate, and thus be sequestered,
406 altering gene expression to permit bacterial adaptation to a specific environment (Schramm *et*
407 *al.*, 2019). Whether high levels of c-di-GMP promote such processes remains to be tested, but
408 c-di-GMP levels certainly alter PlzA binding affinity.

409 Our study sought to identify if PlzA can bind nucleic acids and what role c-di-GMP plays in
410 that function. The data is conclusive that PlzA indeed binds DNA, both double and single-
411 stranded, and RNA, with a preference for the dsDNA and RNA. PlzA also displayed higher
412 affinity for certain nucleic acid types over others, and PlzA-*glp* DNA binding was competed
413 away by specific competitor but not nonspecific competitor. Further, the nucleic acid binding
414 at the *glpFKD* locus by PlzA is dependent on c-di-GMP. A caveat of the data is that the
415 calculated dissociation constants for PlzA-nucleic acids are lower than typically observed for
416 protein-nucleic acid interactions. The higher dissociation constants could be attributed to our
417 method of choice, EMSA, as some potential dissociation and protein aggregation were
418 observed. Attempts were made with various alterations aimed to improve the stability of the
419 complexes during electrophoresis, such as altering the gel percentage, pH of the running
420 buffer, salt/ion concentrations of the reaction buffer, and addition of detergents to the reaction
421 (Hellman and Fried, 2007). Altering the pH of the running buffer to 8.0 decreased the
422 aggregation in the wells but smearing still occurred at higher protein and c-di-GMP
423 concentrations (data not shown). The experimental conditions presented and reported here
424 yielded the most consistent results.

425 PlzA bound to a sequence adjacent to the promoter and extending 35 bp into the 5' UTR of
426 *glpF*. This site has been shown to positively affect *glpFKD* transcript levels and is a site where
427 two other borrelial regulators, SpoVG and BadR, also bind (Grove *et al.*, 2017; Savage *et al.*,
428 2018; Zhang *et al.*, 2022; Saylor *et al.*, 2023). BadR, the *Borrelia* Host Adaption Regulator,
429 has recently been identified as a repressor of *glpFKD*, while PlzA has previously been shown
430 to exert both positive and negative effects on *glpFKD*, at high and low levels of c-di-GMP
431 respectively (Zhang *et al.*, 2018; Zhang *et al.*, 2022). Although SpoVG can bind the DNA and

432 RNA of *glpFKD*, the transcriptional consequences of these interactions are unknown (Savage
433 *et al.*, 2018; Saylor *et al.*, 2023). How PlzA binding affects *glpFKD* expression, and how these
434 proteins work in tandem to regulate glycerol catabolism, is currently being investigated. Multi-
435 layered regulation of glycerol catabolism is found in other bacteria indicating this is not a
436 phenomenon unique to *Borrelia* (Bong *et al.*, 2019).

437 During the preparation of this manuscript, Van Gundy et al. published a report identifying RNA
438 chaperone activity by PlzA (Van Gundy *et al.*, 2023). The authors concluded that this activity
439 is independent of c-di-GMP. This greatly deviates from our results that c-di-GMP is required
440 for nucleic acid binding. This was acknowledged by those authors who suggested that
441 differences in methodologies and conditions might have contributed to the differences in
442 observed results. Some of these differences include their use of non-borrelial derived RNAs,
443 a different PlzA site-mutant, equimolar concentrations of c-di-GMP, and filter binding assays
444 used to calculate dissociation constants. Indeed, the differences in methodology and
445 conditions between the two studies make it difficult to draw comparisons between calculated
446 apparent $K_D$ values, as they are only constant under the given conditions tested (Jarmoskaite
447 *et al.*, 2020). However, some facets of the studies can still be compared. Their study utilized
448 short, unstructured, non-borrelial derived RNAs, while the nucleic acids used in our study are
449 borrelial derived, although examining just one locus PlzA is known to affect. Indeed, our data
450 indicates that PlzA preferentially binds double-stranded/structured nucleic acids. No condition
451 we tested yielded low nanomolar range binding. Regardless, the methodology yielded
452 reproducible data that allowed for the identification of PlzA c-di-GMP-dependent nucleic acid-
453 binding.

454 Given our finding that c-di-GMP levels greatly affect the affinity of PlzA for nucleic acids, we
455 tested binding to both *glpFKD* DNA and RNA under equimolar conditions like those used by
456 Van Gundy et al. In our hands, equimolar concentrations of c-di-GMP yielded significantly
457 reduced nucleic acid binding affinities than those exceeding the calculated $K_D$ of PlzA for c-di-
458 GMP. Considering the higher $K_D$ of the PlzA-c-di-GMP interaction (1.25-6.25 μM), under

459 equimolar conditions reaching the $K_D$ of PlzA-c-di-GMP depends on the protein concentration
460 used. The protein concentrations used in the other study likely never reached a concentration
461 that exceeded the $K_D$ of PlzA for c-di-GMP to saturate half of the PlzA molecules, except at
462 the higher protein ranges tested (1-2 μM). This could explain the observed weaker RNA
463 binding and/or chaperone activity with holo-PlzA.

464 We chose to evaluate saturating c-di-GMP concentrations to evaluate the maximal nucleic
465 acid binding activity of holo-PlzA and mitigate potential variability in the calculated apparent
466 $K_D$ values. It was also never confirmed if their PlzA protein preparations co-purified with c-di-
467 GMP, which could contribute to observed binding in their apo-PlzA conditions. We also did not
468 observe binding under any tested conditions with the $PlzA_{RD\text{-}RD}$ mutant, which cannot bind c-
469 di-GMP. Lastly, the goals for our studies differed greatly as they sought to study RNA
470 chaperone activity, while we set out to investigate PlzA nucleic acid binding at the *glpFKD*
471 operon. Our two studies, however, do corroborate that PlzA can bind RNA and suggest that
472 this function plays a role in the regulation of borrelial gene expression. We agree that further
473 investigation is required to unravel the molecular mechanisms of PlzA's interactions with
474 nucleic acids, and the roles that those interactions play in gene regulation in this important
475 pathogen.

476 It is known that the affinity and specificity of proteins for target nucleic acids are impacted by
477 co-effectors (Carey, 2022). We observed that adding exogenous c-di-GMP increased binding
478 affinity of PlzA for *glp*-derived DNA and RNA. Studies in other bacteria with multiple PilZ
479 domain proteins have suggested that the differential affinity of the various PilZ receptors for c-
480 di-GMP sequentially regulates the processes that respond to c-di-GMP (Pultz *et al.*, 2012;
481 Junkermeier and Hengge, 2023). Given that PlzA is the only PilZ domain protein in most *B.*
482 *burgdorferi* isolates, an alternative to this could be that cellular levels of c-di-GMP alter the
483 affinity and/or specificity of PlzA. We propose a model in which c-di-GMP availability alters the
484 functionality of PlzA, and thus, the targets regulated by PlzA could depend on the c-di-GMP
485 levels available at different stages of the enzootic life cycle (Figure 11).

486 During vertebrate infection, no c-di-GMP is produced, favoring apo-PlzA functions such as
487 RNA chaperone activity (Van Gundy *et al.*, 2023). When c-di-GMP is present, holo-PlzA can
488 also anneal RNAs and potentially interact with RNAP (Grassmann *et al.*, 2023; Van Gundy *et*
489 *al.*, 2023). At lower levels of c-di-GMP, PlzA nucleic-acid binding affinity is low for certain target
490 genes such as *glpFKD*. As c-di-GMP levels increase, such as in a tick or during the blood
491 meal, binding affinity for target nucleic acids is increased and potential multimerization of PlzA
492 molecules on DNA could occur. Lastly, we hypothesize that an unknown signal might regulate
493 PlzA activity at high concentrations resulting in the release of holo-PlzA from target DNAs.
494 This hypothesis requires further investigation, as does overall regulation of c-di-GMP in *B.*
495 *burgdorferi*.

496 In conclusion, PlzA is a c-di-GMP dependent nucleic acid binding protein. While other c-di-
497 GMP binding receptors have been identified as DNA-binding proteins, PlzA is the first that has
498 been demonstrated to also bind RNA, thus expanding the functional diversity of c-di-GMP
499 binding proteins. Given that PlzA can bind to both DNA and RNA, it could have a role in
500 coordinating transcriptional complexes, and it supports the notion that PlzA can interact with
501 RNAP (Grassmann *et al.*, 2023). Our study examined PlzA nucleic-acid binding at a locus
502 known to be affected by PlzA, the *glpFKD* catabolism operon, but sites/ligands of higher affinity
503 could exist. It remains to be seen what additional targets in the *B. burgdorferi*
504 genome/transcriptome fall under the umbrella of the PlzA regulon. Our work identifying PlzA
505 as a novel nucleic acid-binding protein provides a basis for its functional mechanism. This will
506 further inform our understanding of how *B. burgdorferi* regulates gene expression in response
507 to environmental cues and help unravel the PlzA regulon.

508 **MATERIAL AND METHODS**

509 **Routine manipulations and molecular cloning**

510 Oligonucleotides used in this study are listed in Table 2 and were ordered from Integrated
511 DNA Technologies (IDT). *B. burgdorferi* genomic DNA was purified utilizing the E.Z.N.A Tissue

512 DNA kit (OMEGA). Standard and high-fidelity PCR were performed with 2X DreamTaq Green
513 PCR Master Mix (Thermo Scientific) or Q5 High-Fidelity 2X Master Mix (NEB), respectively.
514 Plasmids were isolated using QIAprep Spin Miniprep kits (Qiagen) according to the Miraprep
515 protocol (Pronobis *et al.*, 2016). All plasmid constructs were transformed into chemically
516 competent *E. coli* Top10 (Invitrogen) or DH5α (Invitrogen) strains for cloning and plasmid
517 maintenance. Positive clones were identified by colony PCR screening with the appropriate
518 primers sets, and DNA sequencing was performed by Eurofins Genomics LLC (Louisville, KY).

519 **Plasmid construction**

520 The wild-type (WT) *plzA* gene from *B. burgdorferi* strain B31, was cloned between the
521 NdeI/XhoI sites of pET28a(+) and thus fused in-frame with an amino-terminal 6xHis-tag.
522 Truncated *plzA* genes, named *plzA*-NTD and *plzA*-CTD encoding the N-terminal (residues 1-
523 141) and C-terminal (residues 142-261) domains of PlzA, respectively, were generated via
524 gene synthesis and cloned to produce 6xHis-tagged proteins by Genscript (Piscataway, NJ).
525 Briefly, the synthesized truncations were cloned into the pET28b(+) vector with *plzA*-NTD
526 cloned between the BamHI/NotI sites producing an amino-terminal 6xHis-tag fusion, while
527 *plzA* CTD was cloned between the NcoI/XhoI sites producing a carboxy-terminal 6xHis-tag
528 fusion.

529 **Generation of the site-directed PlzA R145D-R149D double mutant**

530 Site-directed mutagenesis by overlap extension PCR was used to generate a PlzA mutant that
531 cannot bind c-di-GMP. Two-point mutations were introduced into a pTrcHis TOPO (Invitrogen)
532 construct containing the *plzA* gene. The successful introduction of the mutations was
533 confirmed by DNA sequencing. The site-directed PlzA double mutant is denoted as $PlzA_{RD\text{-}RD}$.
534 The oligonucleotide primers used for site-directed mutagenesis are listed in Table 2.

535 **Recombinant protein overexpression and purification**

536 For recombinant protein expression, *E. coli* Rosetta 2(DE3)(pLysS) (Novagen) chemically
537 competent cells were used for $PlzA_{WT}$, $PlzA_{RD-RD}$, and N-terminal PlzA domain ($PlzA_{NTD}$), while
538 One Shot BL21 Star (DE3) cells were used for the C-terminal PlzA domain ($PlzA_{CTD}$).
539 Overnight bacterial cultures were diluted 1:100 into Super broth (tryptone 32 g, yeast extract
540 20 g, NaCl 5 g per liter) supplemented with the appropriate antibiotics (kanamycin-50 µg/ml,
541 carbenicillin-100 µg/ml, and/or chloramphenicol-30 µg/ml). The cultures were allowed to grow
542 to an $OD_{600}$ of 0.5-1.0 and protein expression was subsequently induced by the addition of
543 0.25 mM ($PlzA_{NTD}$ only) or 0.5 mM isopropyl-β-D-thiogalactopyranoside (IPTG). Induced
544 cultures were incubated at either 37°C for 3-4 h ($PlzA_{WT}$ and $PlzA_{CTD}$), 29°C for 4-6 h ($PlzA_{WT}$),
545 or overnight at room temperature ($PlzA_{RD-RD}$ and $PlzA_{NTD}$). The cells were harvested by
546 centrifugation at 5400 x *g* for 30 min at 4°C, and the cell pellets were frozen at -80°C until
547 protein purification.

548 For protein extraction, cell pellets were thawed on ice and resuspended in equilibration buffer
549 (20mM sodium phosphate, 300 mM NaCl, 10 mM imidazole, pH 8.0) and lysed via sonication.
550 Lysates were clarified by centrifugation at 23700 x *g* for 20 min at 4°C, and the supernatant
551 was retained. When further clarification was required due to lysate viscosity, the supernatants
552 were passed through a sterile 0.22 µM Millex-GS Syringe Filter Unit (MilliporeSigma). Protein
553 purification was performed via column affinity chromatography using either HisPur Ni-NTA
554 resin (Thermo Scientific) or the Magne-His purification system (Promega Corporation) for
555 $PlzA_{RD-RD}$ per manufacturer protocol. Eluted protein solutions were dialyzed overnight into
556 EMSA buffer (50 mM Tris-HCl [pH 7.5], 50 mM KCl, 1 mM dithiothreitol (DTT), 1 mM
557 ethylenediaminetetraacetic acid (EDTA) [pH 8.0], 1 mM phenylmethanesulfonyl fluoride
558 (PMSF), 10% glycerol (v/v), and 0.01% Tween-20). The dialyzed proteins were then
559 concentrated using Amicon Ultra 3K ($PlzA_N$ and $PlzA_C$) or 10K ($PlzA_{WT}$ and $PlzA_{RD-RD}$)
560 centrifugal filter units (MilliporeSigma). Aliquots of dialyzed proteins were assessed for purity
561 by SDS-PAGE and Coomassie brilliant blue staining. Final recombinant protein concentrations
562 were determined using Quick Start Bradford Protein Assays (Bio-Rad) with bovine serum

563 albumin as the reference protein for standard curves. Purified protein aliquots were stored at
564 -80°C.

565 **Nucleic acid fragments design and generation**

566 All probe sequences were derived from the genomic sequence of *B. burgdorferi* type strain
567 B31, and the corresponding primers are reported in Table 2 (Fraser *et al.*, 1997; Casjens *et*
568 *al.*, 2000). Large and small DNA substrates were used in this study. Larger fluorescently
569 tagged fragments >60 bp were generated by PCR amplification of the target sequences from
570 B31 genomic DNA and subsequent cloning into the pCR 2.1 TA vector (Invitrogen) following
571 TOPO TA protocols. Subsequently, target-specific or M13 F and R IRDye 800-labeled primers
572 were used for PCR of the plasmid templates to produce labeled DNA fragments for binding
573 studies. All PCR-generated probes were treated with exonuclease I (NEB) according to the
574 manufacturer's protocol to remove single-stranded DNA, followed by ethanol precipitation.
575 The DNA was resuspended in molecular-grade water (Ambion) and quantified by Nanodrop
576 UV spectrometry.

577 Smaller probes <60 bp long were produced by annealing complementary unlabeled and IRDye
578 800-labeled oligonucleotides at equimolar concentrations at 95°C for 5 min and were gradually
579 cooled overnight at RT. All probes were aliquoted and stored at -20°C until further use.
580 Unlabeled and 5' IRDye 800 (LI-COR Biosciences) labeled oligonucleotides were synthesized
581 by IDT. Alexa Fluor 488 conjugated RNA probes corresponding to the transcribed regions of
582 the respective DNA probes were also synthesized by IDT.

583 **Electrophoretic mobility shift assays (EMSA)**

584 EMSA reactions were performed in EMSA buffer at RT with a final concentration of dsDNA
585 probe of 10 nM or RNA probe of either 10 nM or 50 nM. EMSA reaction mixtures were
586 supplemented with 3'5' c-di-GMP (Sigma-Aldrich) at various concentrations ranging from 0 to
587 100 μM. c-di-GMP was not added to the gel or running buffer. Experiments using equimolar
588 concentrations of c-di-GMP are relative to the final protein concentration in the reaction.

589 Proteins were co-incubated with c-di-GMP for 5 min before the addition of any nucleic acids.
590 Prior to the addition of labeled probe, the non-specific competitor poly-dI-dC (Roche) was
591 added to the EMSA reactions at a final concentration of 2.5 ng/μL, and the reaction mix was
592 allowed to incubate another 5 min (Larouche *et al.*, 1996). Labeled probes were added last,
593 and the reactions were subsequently incubated for an additional 10 min prior to loading onto
594 gels. Competition EMSAs were conducted similarly but with the unlabeled, specific competitor
595 added after poly-dI-dC and then allowed to incubate with the reaction prior to the addition of
596 the labeled probe. Regarding RNA EMSAs, when RNase contamination was evident in
597 recombinant protein preparations, RiboGuard (Lucigen) or SUPERase•In (Ambion) RNase
598 inhibitor was added to the EMSA mixtures before the addition of RNA to a final concentration
599 of 4 U/μL and 2 U/μL respectively to inhibit RNase activity. The final reaction volume was 10
600 μL prior to the addition of loading dye.

601 For visualization during electrophoresis, 2 μL of EMSA loading dye (0.8 mg/mL Orange G, 15
602 mg/mL Ficoll 400) was added to each reaction prior to gel loading. Novex TBE 6 or 10% gels
603 (Invitrogen) were pre-run in 0.5x TBE running buffer (pH ~8.4 +/- 0.5), at 100V for a minimum
604 of 30 min. Due to the complexes of the larger *glpFKD*(-219) probe and higher concentrations
605 of PlzA not exiting the well, the pH of the running buffer was adjusted to a pH of 8.0
606 immediately prior to electrophoresis which allowed the complexes to enter the gel matrix. The
607 pH was not adjusted for EMSAs using nucleic acid fragments <60 bp as complexes readily
608 exited the well at the standard pH of 0.5x TBE running buffer. The entire reaction mixture was
609 then loaded onto the pre-run gels and resolved at 100 V for 60-90 min at RT. EMSA images
610 were acquired with a ChemiDoc Imaging System (Bio-Rad).

611 **Densitometry and statistics**

612 Densitometry of EMSAs was performed using Image Lab 6.1 (Bio-Rad) software. Analyses
613 were performed on triplicate EMSAs. Lanes as well as free and shifted bands were added
614 manually, and intensity values were reported as band percentage. For dsDNA EMSAs, free

615 dsDNA band percentages were normalized to the probe only control band percentage. The
616 free DNA band percentage values were then used to determine the percent shifted of the
617 respective probe relative to the free probe. For RNA and ssDNA EMSAs, lanes and bands
618 were selected manually, and the shifted bands were analyzed to obtain the percent shifted
619 values. Probe signal stuck in the gel wells, attributed to potential protein aggregation, were
620 not considered shifts, and thus omitted from densitometric analysis.

621 To calculate the apparent dissociation constant ($K_D$), nonlinear regression analysis was
622 performed to determine the best-fit values for each experimental condition tested. Briefly,
623 protein concentrations were plotted against the shifted band percentage values obtained from
624 densitometry using the one-site specific binding setting in Prism GraphPad 9.5.1. Confidence
625 was set at 95% with the analysis considering each replicate value from triplicate EMSAs
626 performed for the analysis. Either a Welch's t-test or Welch ANOVA followed by a Dunnett's
627 T3 multiple comparisons test, was used to compare fits.

628 **Docking analysis and protein modeling**

629 Computational modeling of holo-PlzA (PDB ID: 7mie) in complex with the nucleic acids of
630 interest was performed using the HDOCK server: http://hdock.phys.hust.edu.cn/. Briefly, the
631 PDB and chain ID of PlzA was entered for the input receptor molecule to retrieve the crystal
632 structure of the protein for the analysis. For each analysis, the corresponding nucleic acid
633 sequence of interest was then pasted as the input ligand molecule, and the type of nucleic
634 acid selected from the drop-down menu. The input nucleic acid sequences are listed in Table
635 2. All analyses were performed with default parameters. The top model for each computation
636 is shown. Docking and confidence scores are provided in the corresponding figure legends.
637 The more negative the docking score, the more probable the binding. A confidence score
638 above 0.7 indicates the molecules would be highly likely to bind.

639 Protein structure prediction for $PlzA_{NTD}$, $PlzA_{CTD}$, and $PlzA_{RD\text{-}RD}$ was performed via AlphaFold.
640 All output PDB files generated from the various analyses were viewed with ChimeraX 1.4
641 (Goddard *et al.*, 2018; Jumper *et al.*, 2021; Pettersen *et al.*, 2021).

642 **Cyclic di-nucleotide LC-MS analysis**

643 Detection of cyclic di-nucleotides in recombinant protein purifications was conducted by liquid
644 chromatography-tandem mass spectrometry (LC-MS/MS) at the Michigan State University
645 Mass Spectrometry core. Briefly, recombinant proteins were purified and quantified as
646 mentioned previously and subsequently dialyzed into EMSA buffer without Tween-20. For LC-
647 MS/MS analysis, approximately 1 mg/mL of $PlzA_{WT}$, $PlzA_{RD\text{-}RD,}$ $PlzA_{NTD}$, and $PlzA_{CTD}$ were
648 aliquoted and stored at -80°C until shipment to the core facility. Nucleotides bound to purified
649 protein samples (1mg/mL) were analyzed by precipitating protein with 3 volumes of acetonitrile
650 followed by centrifugation to pellet precipitated protein. The supernatant was transferred to a
651 new tube and evaporated to dryness. The sample was reconstituted in mobile phase solvent
652 A (10 mM tributylamine + 15 mM acetic acid in water/methanol, 97:3 v/v). LC-MS analysis was
653 performed on a Waters Xevo G2-XS Quadrupole-Time-of-Flight (QTof) mass spectrometer
654 interfaced with a Waters Acquity UPLC system. 10 µL of sample was injected onto a Waters
655 Acquity BEH-C18 UPLC column (2.1x50 mm) and compounds were separated using the
656 following gradient: initial conditions were 100% mobile phase A, hold at 100% A until 1 min,
657 ramp to 99% B at 7 min (mobile phase B: methanol), hold at 99% B until 8 min, return to 100%
658 A at 8.01 min and hold until 10 min. The flow rate through the column was 0.3 ml/min and the
659 column temperature was held at 40°C. Compounds were ionized by electrospray ionization
660 operated in negative mode. Capillary voltage was 2.0 kV, cone voltage was 35, source
661 temperature was 100C and desolvation temperature was 350C. The cone gas and desolvation
662 gas flows were 50 L/hr and 600 L/hr respectively. A TOF MS scan method with targeted
663 enhancement of m/z 689 was used with 0.5 second scan time. Lockmass correction was
664 performed using leucine enkephalin as the reference compound.

665 Data were processed using Waters Masslynx software. Extracted ion chromatograms were
666 performed to look for the presence of c-di-GMP (m/z 689.09), c-di-AMP (m/z 657.09) and c-
667 GAMP (673.09). The intensity values were converted to relative abundance as determined
668 from the base peak values. The c-di-GMP concentration was determined from the peak area
669 of the target compound against a standard curve of known c-di-GMP concentrations. These
670 concentrations were calculated using the Targetlynx tool in the Waters Masslynx software.
671 The percentage of protein bound with c-di-GMP was calculated from the total protein and
672 calculated c-di-GMP concentrations in each sample.

673 **Circular dichroism spectroscopy**

674 The CD analysis was performed on $PlzA_{WT}$, $PlzA_{RD\text{-}RD}$, $PlzA_{NTD}$, and $PlzA_{CTD}$ in EMSA dialysis
675 buffer (detailed above) at the University of Kentucky Center for Molecular Medicine Protein
676 Core. Briefly, 400 µL of each protein solution at a concentration of 180-210 µg/mL was pipetted
677 into a 1 mm quartz cuvette and loaded into a Jasco J-810 spectrophotometer. The samples
678 were scanned at 0.1 nm increments and CD spectra collected for wavelengths 200-260 nM.
679 EMSA buffer alone or supplemented with 50 µM c-di-GMP were also analyzed and used as
680 controls. Data were visualized in GraphPad Prism 9.5.1.

681 **AVAILABILITY**

682 HDOCK (http://hdock.phys.hust.edu.cn/)

683 **ACKNOWLEDGEMENT**

684 We dedicate this manuscript to our friend and colleague Christina R. Savage, Ph.D., whose
685 initial studies on PlzA were invaluable to this work. We also thank Jessamyn Moore and
686 Tatiana Castro Padovani for their support of the studies undertaken. Circular Dichroism was
687 performed at the University of Kentucky Center for Molecular Medicine Protein Core, and we
688 thank Martin Chow for his assistance on these studies. The LC-MS/MS to detect di-nucleotides
689 was performed by the Mass Spectrometry and Metabolomics Core at Michigan State

690 University. A sincere thank you to Tony Schilmiller at MSU for all his help with the mass
691 spectrometry services. Figures 1, 3a, 5a, 8a and 11 were created via BioRender.

692 **FUNDING**

693 Funding for open access charge: US National Institutes of Health (grant R01 AI144126-3 to
694 B.S.).

695 **CONFLICT OF INTEREST**

696 None declared.

697 **REFERENCES**

698 Adams, P.P., Avile, C.F., Popitsch, N., Bilusic, I., Schroeder, R., Lybecker, M., and
699 Jewett, M.W. (2017) In vivo expression technology and 5′ end mapping of the *Borrelia*
700 *burgdorferi* transcriptome identify novel RNAs expressed during mammalian infection.
701 *Nucleic Acids Res* **45**: 775–792.

702 Amikam, D., and Galperin, M.Y. (2006) PilZ domain is part of the bacterial c-di-GMP
703 binding protein. *Bioinformatics* **22**: 3–6
704 https://academic.oup.com/bioinformatics/article/22/1/3/218448. Accessed February 18,
705 2022.

706 Babb, K., Bykowski, T., Riley, S.P., Miller, M.C., Demoll, E., and Stevenson, B. (2006)
707 *Borrelia burgdorferi* EbfC, a novel, chromosomally encoded protein, binds specific DNA
708 sequences adjacent to erp loci on the spirochete's resident cp32 prophages. *J Bacteriol*
709 **188**: 4331–4339 https://journals.asm.org/journal/jb. Accessed April 8, 2022.

710 Bauer, W.J., Luthra, A., Zhu, G., Radolf, J.D., Malkowski, M.G., and Caimano, M.J.
711 (2015) Structural characterization and modeling of the *Borrelia burgdorferi* hybrid
712 histidine kinase Hk1 periplasmic sensor: A system for sensing small molecules
713 associated with tick feeding. *J Struct Biol* **192**: 48–58.

714 Bong, H.J., Ko, E.M., Song, S.Y., Ko, I.J., and Oh, J. Il (2019) Tripartite regulation of
715 the *glpFKD* operon involved in glycerol catabolism by gylr, crp, and sigf in
716 *Mycobacterium smegmatis*. *J Bacteriol* **201**.

717 Burns, L.H., Adams, C.A., Riley, S.P., Jutras, B.L., Bowman, A., Chenail, A.M., *et al.*
718 (2010) BpaB, a novel protein encoded by the Lyme disease spirochete's cp32
719 prophages, binds to *erp* Operator 2 DNA. *Nucleic Acids Res* **38**: 5443–5455.

720 Caimano, M.J., Dunham-Ems, S., Allard, A.M., Cassera, M.B., Kenedy, M., and Radolf,
721 J.D. (2015) Cyclic di-GMP modulates gene expression in Lyme disease spirochetes at
722 the tick-mammal interface to promote spirochete survival during the blood meal and

723 tick-to-mammal transmission. *Infect Immun* **83**: 3043–3060 http://dx.doi.org/10.1128.
724 Accessed May 1, 2021.

725 Caimano, M.J., Kenedy, M.R., Kairu, T., Desrosiers, D.C., Harman, M., Dunham-Ems,
726 S., *et al.* (2011) The hybrid histidine kinase Hk1 is part of a two-component system that
727 is essential for survival of *Borrelia burgdorferi* in feeding *Ixodes scapularis* ticks. *Infect*
728 *Immun* **79**: 3117–3130 http://www.ncbi.nlm.nih.gov/Structure/cdd/cdd.shtml. Accessed
729 February 13, 2022.

730 Carey, J. (2022) Affinity, Specificity, and Cooperativity of DNA Binding by Bacterial
731 Gene Regulatory Proteins. *Int J Mol Sci* **23**: 1–16.

732 Casjens, S., Palmer, N., Vugt, R. Van, Huang, W.M., Stevenson, B., Rosa, P., *et al.*
733 (2000) A bacterial genome in flux: The twelve linear and nine circular
734 extrachromosomal DNAs in an infectious isolate of the Lyme disease spirochete
735 *Borrelia burgdorferi*. *Mol Microbiol* **35**: 490–516.

736 Cheang, Q.W., Xin, L., Chea, R.Y.F., and Liang, Z.X. (2019) Emerging paradigms for
737 PilZ domain-mediated C-di-GMP signaling. *Biochem Soc Trans* **47**: 381–388.

738 Chou, S.H., and Galperin, M.Y. (2016) Diversity of cyclic di-GMP-binding proteins and
739 mechanisms. *J Bacteriol* **198**: 32–46 http://ncbi.nlm.nih.gov/Complete_Genomes/c-di-
740 GMP.html. Accessed February 13, 2022.

741 Corona, A., and Schwartz, I. (2015) *Borrelia burgdorferi* : Carbon Metabolism and the
742 Tick-Mammal Enzootic Cycle. *Microbiol Spectr* **3**.

743 Fraser, C.M., Casjens, S., Huang, W.M., Sutton, G.G., Clayton, R., Lathigra, R., *et al.*
744 (1997) Genomic sequence of a Lyme disease spirochaete, *Borrelia burgdorferi*. *Nature*
745 **390**: 580–586.

746 Freedman, J.C., Rogers, E.A., Kostick, J.L., Zhang, H., Iyer, R., Schwartz, I., and
747 Marconi, R.T. (2009) Identification and molecular characterization of a cyclic-di-GMP
748 effector protein, PlzA (BB0733): Additional evidence for the existence of a functional
749 cyclic-di-GMP regulatory network in the Lyme disease spirochete, *Borrelia burgdorferi*.
750 *FEMS Immunol Med Microbiol* **58**: 285–294
751 https://academic.oup.com/femspd/article/58/2/285/597665. Accessed April 26, 2021.

752 Fried, M., and Crothers, D.M. (1981) Equilibria and kinetics of lac repressor-operator
753 interactions by polyacrylamide gel electrophoresis. *Nucleic Acids Res* **9**: 1981.

754 Fried, M.G. (1989) Measurement of protein-DNA interaction parameters by
755 electrophoresis mobility shift assay. *Electrophoresis* **10**: 366–376.

756 Galperin, M.Y., and Chou, S.H. (2020) Structural conservation and diversity of PilZ-
757 related domains. *J Bacteriol* **202**.

758 Galperin, M.Y., Nikolskaya, A.N., and Koonin, E. V. (2001) Novel domains of the
759 prokaryotic two-component signal transduction systems. *FEMS Microbiol Lett* **203**: 11–
760 21 https://academic.oup.com/femsle/article/203/1/11/478433. Accessed March 17,
761 2022.

762 Goddard, T.D., Huang, C.C., Meng, E.C., Pettersen, E.F., Couch, G.S., Morris, J.H.,
763 and Ferrin, T.E. (2018) UCSF ChimeraX: Meeting modern challenges in visualization
764 and analysis. *Protein Science* **27**: 14–25.

765 Grassmann, A.A., Tokarz, R., Golino, C., McLain, M.A., Groshong, A.M., Radolf, J.D.,
766 and Caimano, M.J. (2023) BosR and PlzA reciprocally regulate RpoS function to
767 sustain *Borrelia burgdorferi* in ticks and mammals. *Journal of Clinical Investigation*
768 http://www.jci.org/articles/view/166710.

769 Groshong, A.M., Grassmann, A.A., Luthra, A., Mclain, M.A., Provatas, A.A., Radolf,
770 J.D., and Caimano, M.J. (2021) PlzA is a bifunctional c-di-GMP biosensor that
771 promotes tick and mammalian host- adaptation of *Borrelia burgdorferi*. *PLoS Pathog*
772 **17**: 1–31.

773 Grove, A.P., Liveris, D., Iyer, R., Petzke, M., Rudman, J., Caimano, M.J., *et al.* (2017)
774 Two Distinct Mechanisms govern RpoS-Mediated Repression of Tick-Phase Genes
775 during Mammalian Host Adaptation by *Borrelia burgdorferi*, the Lyme Disease
776 Spirochete. *mBio* **8** https://journals.asm.org/doi/full/10.1128/mBio.01204-17. Accessed
777 June 18, 2022.

778 He, M., Ouyang, Z., Troxell, B., Xu, H., Moh, A., Piesman, J., *et al.* (2011) Cyclic di-gmp
779 is essential for the survival of the lyme disease spirochete in ticks. *PLoS Pathog* **7**.

780 He, M., Zhang, J.J., Ye, M., Lou, Y., and Yang, X.F. (2014) Cyclic Di-GMP receptor
781 PlzA controls virulence gene expression through RpoS in *Borrelia burgdorferi*. *Infect*
782 *Immun* **82**: 445–452 http://iai.asm.org/. Accessed April 26, 2021.

783 Helble, J.D., McCarthy, J.E., and Hu, L.T. (2021) Interactions between *Borrelia*
784 *burgdorferi* and its hosts across the enzootic cycle. *Parasite Immunol* **43**.

785 Hellman, L.M., and Fried, M.G. (2007) Electrophoretic mobility shift assay (EMSA) for
786 detecting protein-nucleic acid interactions. *Nat Protoc* **2**: 1849–1861.

787 Hengge, R. (2009) Principles of c-di-GMP signalling in bacteria. *Nat Rev Microbiol* **7**:
788 263–273.

789 Hsieh, M.L., Hinton, D.M., and Waters, C.M. (2018) VpsR and cyclic di-GMP together
790 drive transcription initiation to activate biofilm formation in *Vibrio cholerae*. *Nucleic*
791 *Acids Res* **46**: 8876–8887.

792 Huang, S.Y., and Zou, X. (2014) A knowledge-based scoring function for protein-RNA
793 interactions derived from a statistical mechanics-based iterative method. *Nucleic Acids*
794 *Res* **42**.

795 Jarmoskaite, I., Alsadhan, I., Vaidyanathan, P.P., and Herschlag, D. (2020) How to
796 measure and evaluate binding affinities. *Elife* **9**: 1–34.

797 Jenal, U., Reinders, A., and Lori, C. (2017) Cyclic di-GMP: Second messenger
798 extraordinaire. *Nat Rev Microbiol* **15**: 271–284
799 http://dx.doi.org/10.1038/nrmicro.2016.190.

800 Jumper, J., Evans, R., Pritzel, A., Green, T., Figurnov, M., Ronneberger, O., *et al.*
801 (2021) Highly accurate protein structure prediction with AlphaFold. *Nature* **596**: 583–
802 589 http://dx.doi.org/10.1038/s41586-021-03819-2.

803 Junkermeier, E.H., and Hengge, R. (2023) Local signaling enhances output specificity
804 of bacterial c-di-GMP signaling networks. *microLife* **4**.

805 Jutras, B.L., Bowman, A., Brissette, C.A., Adams, C.A., Verma, A., Chenail, A.M., and
806 Stevenson, B. (2012) EbfC (YbaB) is a new type of bacterial nucleoid-associated
807 protein and a global regulator of gene expression in the Lyme disease spirochete. *J*
808 *Bacteriol* **194**: 3395–3406.

809 Jutras, B.L., Chenail, A.M., Carroll, D.W., Miller, M.C., Zhu, H., Bowman, A., and
810 Stevenson, B. (2013a) Bpur, the Lyme disease spirochete's PUR domain protein:
811 Identification as a transcriptional modulator and characterization of nucleic acid
812 interactions. *Journal of Biological Chemistry* **288**: 26220–26234 http://www.jbc.org/.
813 Accessed October 5, 2020.

814 Jutras, B.L., Chenail, A.M., Rowland, C.L., Carroll, D., Miller, M.C., Bykowski, T., and
815 Stevenson, B. (2013b) Eubacterial SpoVG Homologs Constitute a New Family of Site-
816 Specific DNA-Binding Proteins. *PLoS One* **8**: 66683 www.plosone.org. Accessed April
817 26, 2021.

818 Kim, B., and Little, J.W. (1992) Dimerization of a specific DNA-binding protein on the
819 DNA. *Science (1979)* **255**: 203–206.

820 Kohler, J.J., Metallo, S.J., Schneider, T.L., and Schepartz, A. (1999) DNA specificity
821 enhanced by sequential binding of protein monomers. *Proc Natl Acad Sci U S A* **96**:
822 11735–11739.

823 Kostick, J.L., Szkotnicki, L.T., Rogers, E.A., Bocci, P., Raffaelli, N., and Marconi, R.T.
824 (2011) The diguanylate cyclase, Rrp1, regulates critical steps in the enzootic cycle of
825 the Lyme disease spirochetes. *Mol Microbiol* **81**: 219–231
826 https://onlinelibrary.wiley.com/doi/full/10.1111/j.1365-2958.2011.07687.x. Accessed
827 April 15, 2022.

828 Kostick-Dunn, J.L., Izac, J.R., Freedman, J.C., Szkotnicki, L.T., Oliver, L.D., and
829 Marconi, R.T. (2018) The *Borrelia burgdorferi* c-di-GMP Binding Receptors, PlzA and
830 PlzB, Are Functionally Distinct. *Front Cell Infect Microbiol* **8**: 213 www.frontiersin.org.
831 Accessed April 26, 2021.

832 Krusenstjerna, A.C., Arnold, W.K., Saylor, T.C., Tucker, J.S., and Stevenson, B. (2023)
833 *Borrelia* burgdorferi DnaA and the nucleoid-associated protein EbfC coordinate
834 expression of the *dnaX-ebfC* operon. *J Bacteriol* **205**: e00396-22
835 https://doi.org/10.1128/jb.00396-22.

836 Larouche, K., Bergeron, M.-J., Leclerc, S., and Guerin, S. (1996) Optimization of
837 competitor poly(dI-dC).poly(dI-dC) levels is advised in DNA-protein interaction studies
838 involving enriched nuclear proteins. *Biotechniques* **20**: 439–444.

Lee, R.E., and Baust, J.G. (1987) Cold-Hardiness in the Antarctic Tick, *Ixodes uriae*. *Physiol Zool* **60**: 499–506 https://about.jstor.org/terms.

Mallory, K.L., Miller, D.P., Oliver, L.D., Freedman, J.C., Kostick-Dunn, J.L., Carlyon, J.A., *et al.* (2016) Cyclic-di-GMP binding induces structural rearrangements in the PlzA and PlzC proteins of the Lyme disease and relapsing fever spirochetes: A possible switch mechanism for c-di-GMP-mediated effector functions. *Pathog Dis* **74**: 1–8.

Novak, E.A., Sultan, S.Z., and Motaleb, M.A. (2014) The cyclic-di-GMP signaling pathway in the Lyme disease spirochete, *Borrelia burgdorferi*. *Front Cell Infect Microbiol* **4** www.frontiersin.org. Accessed April 26, 2021.

Pappas, C.J., Iyer, R., Petzke, M.M., Caimano, M.J., Radolf, J.D., and Schwartz, I. (2011) *Borrelia burgdorferi* requires glycerol for maximum fitness during the tick phase of the enzootic cycle. *PLoS Pathog* **7**.

Pettersen, E.F., Goddard, T.D., Huang, C.C., Meng, E.C., Couch, G.S., Croll, T.I., *et al.* (2021) UCSF ChimeraX: Structure visualization for researchers, educators, and developers. *Protein Science* **30**: 70–82.

Pitzer, J.E., Syed, S.Z., Hayakawa, Y., Hobbs, G., Miller, M.R., and Motaleb, M.A. (2011) Analysis of the *Borrelia burgdorferi* Cyclic-di-GMP-Binding Protein PlzA Reveals a Role in Motility and Virulence. *Infect Immun* **79**: 1815–1825 http://iai.asm.org/. Accessed April 26, 2021.

Pronobis, M.I., Deuitch, N., and Peifer, M. (2016) The Miraprep: A protocol that uses a Miniprep kit and provides Maxiprep yields. *PLoS One* **11**: 1–12.

Pultz, I.S., Christen, M., Kulasekara, H.D., Kennard, A., Kulasekara, B., and Miller, S.I. (2012) The response threshold of Salmonella PilZ domain proteins is determined by their binding affinities for c-di-GMP. *Mol Microbiol* **86**: 1424–1440.

Riley, S.P., Bykowski, T., Cooley, A.E., Burns, L.H., Babb, K., Brissette, C.A., *et al.* (2009) *Borrelia burgdorferi* EbfC defines a newly-identified, widespread family of bacterial DNA-binding proteins. *Nucleic Acids Res* **37**: 1973–1983 http://www.rcsb.org/. Accessed April 8, 2022.

Rogers, E.A., Terekhova, D., Zhang, H.-M.M., Hovis, K.M., Schwartz, I., and Marconi, R.T. (2009) Rrp1, a cyclic-di-GMP-producing response regulator, is an important regulator of *Borrelia burgdorferi* core cellular functions. *Mol Microbiol* **71**: 1551–1573 http://www.pubmedcentral.nih.gov/articlerender.fcgi?artid=2843504&tool=pmcentrez&rendertype=abstract. Accessed February 18, 2022.

Romling, U., Galperin, M.Y., and Gomelsky, M. (2013) Cyclic di-GMP: the First 25 Years of a Universal Bacterial Second Messenger. *Microbiology and Molecular Biology Reviews* **77**: 1–52.

Rooman, M., Lié Vin, J., Buisine, E., and Wintjens, R. (2002) Cation-p/H-bond Stair Motifs at Protein-DNA Interfaces. *J Mol Biol* **319**: 67–76 http://www.idealibrary.com.

877 Ryjenkov, D.A., Simm, R., Römling, U., and Gomelsky, M. (2006) The PilZ domain is a
878 receptor for the second messenger c-di-GMP: The PilZ domain protein YcgR controls
879 motility in enterobacteria. *Journal of Biological Chemistry* **281**: 30310–30314.

880 Ryjenkov, D.A., Tarutina, M., Moskvin, O. V., and Gomelsky, M. (2005) Cyclic
881 diguanylate is a ubiquitous signaling molecule in bacteria: Insights into biochemistry of
882 the GGDEF protein domain. *J Bacteriol* **187**: 1792–1798
883 https://journals.asm.org/doi/abs/10.1128/JB.187.5.1792-1798.2005. Accessed March
884 17, 2022.

885 Sarenko, O., Klauck, G., Wilke, F.M., Pfiffer, V., Richter, A.M., Herbst, S., *et al.* (2017)
886 More than enzymes that make or break cyclic Di-GMP—local signaling in the
887 interactome of GGDEF/EAL domain proteins of Escherichia coli. *mBio* **8**.

888 Sathyapriya, R., and Vishveshwara, S. (2004) Interaction of DNA with clusters of amino
889 acids in proteins. *Nucleic Acids Res* **32**: 4109–4118.

890 Savage, C.R., Jutras, B.L., Bestor, A., Tilly, K., Rosa, P.A., Tourand, Y., *et al.* (2018)
891 *Borrelia burgdorferi* SpoVG DNA- and RNA-binding protein modulates the physiology of
892 the Lyme disease spirochete. *J Bacteriol* **200** http://jb.asm.org/. Accessed April 26,
893 2021.

894 Saylor, T.C., Savage, C.R., Krusenstjerna, A.C., Jusufovic, N., Zückert, W.R., Brissette,
895 C.A., *et al.* (2023) Quantitative analyses of interactions between SpoVG and RNA/DNA.
896 *Biochem Biophys Res Commun* **654**: 40–46.

897 Schäper, S., Steinchen, W., Krol, E., Altegoer, F., Skotnicka, D., Søgaard-Andersen, L.,
898 *et al.* (2017) AraC-like transcriptional activator CuxR binds c-di-GMP by a PilZ-like
899 mechanism to regulate extracellular polysaccharide production. *Proc Natl Acad Sci U S*
900 *A* **114**: E4822–E4831.

901 Schramm, F.D., Schroeder, K., and Jonas, K. (2019) Protein aggregation in bacteria.
902 *FEMS Microbiol Rev* **44**: 54–72.

903 Singh, A., Izac, J.R., Schuler, E.J.A., Patel, D.T., Davies, C., and Marconi, R.T. (2021)
904 High-resolution crystal structure of the *Borreliella burgdorferi* PlzA protein in complex
905 with c-di-GMP: new insights into the interaction of c-di-GMP with the novel xPilZ
906 domain. *Pathog Dis* **79**: 1–9.

907 Skotnicka, D., Steinchen, W., Szadkowski, D., Cadby, I.T., Lovering, A.L., Bange, G.,
908 and Søgaard-Andersen, L. (2020) CdbA is a DNA-binding protein and c-di-GMP
909 receptor important for nucleoid organization and segregation in *Myxococcus xanthus*.
910 *Nat Commun* **11** https://doi.org/10.1038/s41467-020-15628-8. Accessed February 13,
911 2022.

912 Sultan, S.Z., Pitzer, J.E., Boquoi, T., Hobbs, G., Miller, M.R., and Motaleb, M.A. (2011)
913 Analysis of the HD-GYP domain cyclic dimeric gmp phosphodiesterase reveals a role in
914 motility and the enzootic life cycle of *Borrelia burgdorferi*. *Infect Immun* **79**: 3273–3283.

915 Sultan, S.Z., Pitzer, J.E., Miller, M.R., and Motaleb, M.A. (2010) Analysis of a *Borrelia*
916 *burgdorferi* phosphodiesterase demonstrates a role for cyclic-di-guanosine
917 monophosphate in motility and virulence. *Mol Microbiol* **77**: 128–142.

918 Tan, J.W.H., Wilksch, J.J., Hocking, D.M., Wang, N., Srikhanta, Y.N., Tauschek, M., *et*
919 *al.* (2015) Positive Autoregulation of *mrkHI* by the Cyclic Di-GMP-Dependent MrkH
920 Protein in the Biofilm Regulatory Circuit of *Klebsiella pneumoniae*. *J Bacteriol* **197**:
921 1659–1667.

922 Tschowri, N., Schumacher, M.A., Schlimpert, S., Chinnam, N.B., Findlay, K.C.,
923 Brennan, R.G., and Buttner, M.J. (2014) Tetrameric c-di-GMP mediates effective
924 transcription factor dimerization to control *Streptomyces* development. *Cell* **158**: 1136–
925 1147 http://dx.doi.org/10.1016/j.cell.2014.07.022.

926 Valentini, M., and Filloux, A. (2019) Multiple roles of c-di-GMP signaling in bacterial
927 pathogenesis. *Annu Rev Microbiol* **73**: 387–406.

928 Van Gundy, T., Patel, D., Bowler, B.E., Rothfuss, M.T., Hall, A.J., Davies, C., *et al.*
929 (2023) c-di-GMP regulates activity of the PlzA RNA chaperone from the Lyme disease
930 spirochete. *Mol Microbiol* **119**: 711–727.

931 Wang, F., He, Q., Su, K., Gao, F., Huang, Y., Lin, Z., *et al.* (2016) The PilZ domain of
932 MrkH represents a novel DNA binding motif. *Protein Cell* **7**: 766–772
933 /pmc/articles/PMC5055493/. Accessed February 13, 2022.

934 Wilksch, J.J., Yang, J., Clements, A., Gabbe, J.L., Short, K.R., Cao, H., *et al.* (2011)
935 MrkH, a Novel c-di-GMP-Dependent Transcriptional Activator, Controls *Klebsiella*
936 *pneumoniae* Biofilm Formation by Regulating Type 3 Fimbriae Expression. *PLoS*
937 *Pathog* **7**: e1002204
938 https://journals.plos.org/plospathogens/article?id=10.1371/journal.ppat.1002204.
939 Accessed February 14, 2022.

940 Yan, Y., Tao, H., He, J., and Huang, S.Y. (2020) The HDOCK server for integrated
941 protein–protein docking. *Nat Protoc* **15**: 1829–1852.

942 Yan, Y., Wen, Z., Wang, X., and Huang, S.Y. (2017a) Addressing recent docking
943 challenges: A hybrid strategy to integrate template-based and free protein-protein
944 docking. *Proteins: Structure, Function and Bioinformatics* **85**: 497–512.

945 Yan, Y., Zhang, D., Zhou, P., Li, B., and Huang, S.Y. (2017b) HDOCK: A web server for
946 protein-protein and protein-DNA/RNA docking based on a hybrid strategy. *Nucleic*
947 *Acids Res* **45**: W365–W373.

948 Yang, J., Wilksch, J.J., Tan, J.W.H., Hocking, D.M., Webb, C.T., Lithgow, T., *et al.*
949 (2013) Transcriptional activation of the *mrkA* promoter of the *Klebsiella pneumoniae*
950 type 3 fimbrial operon by the c-di-GMP-dependent MrkH protein. *PLoS One* **8**.

951 Zamorano-Sánchez, D., Fong, J.C.N., Kilic, S., Erill, I., and Yildiz, F.H. (2015)
952 Identification and characterization of VpsR and VpsT binding sites in *Vibrio cholerae*. *J*
953 *Bacteriol* **197**: 1221–1235 http://dx.doi.org/10.1128. Accessed May 2, 2021.

954 Zhang, J.J., Chen, T., Yang, Y., Du, J., Li, H., Troxell, B., *et al.* (2018) Positive and
955 Negative Regulation of Glycerol Utilization by the c-di-GMP Binding Protein PlzA in
956 *Borrelia burgdorferi*. *J Bacteriol* **200** https://doi.org/10.1128/JB. Accessed April 14,
957 2021.

958 Zhang, J.J., Ranghunandanan, S., Wang, Q., Lou, Y., and Yang, X.F. (2022)
959 Mechanism of repression of the glycerol utilization operon in *Borrelia burgdorferi*.
960 *bioRxiv* **PREPRINT:NOT PEER REVIEWED**

961

962 **FIGURES LEGENDS**

963 **FIGURE 1** The *glpFKD* operon, 5' UTR, and designed probe schematic. The glycerol
964 catabolism gene operon (*glpFKD*) contains four genes: *glpF* (BB_0240, glycerol uptake
965 facilitator protein), *glpK* (BB_0241, glycerol kinase), BB_0242 (hypothetical protein), and *glpD*
966 (BB_0243, glycerol-3-phosphate dehydrogenase). The promoter and transcriptional
967 boundaries were previously mapped (Grove *et al.*, 2017). The -35 and -10 sites are bolded
968 and underlined. The transcriptional start site nucleotide is highlighted in blue and topped with
969 an arrow indicating the direction of transcription. The start of the *glpF* ORF is marked by the
970 bolded ATG, while the start of the upstream BB_0239 ORF is labeled, and its nucleotides are
971 italicized. The long arrows indicate the location of primers used to generate a large probe
972 incorporating the entire intergenic region which is denoted as *glpFKD*(-219) for initial DNA
973 binding studies.

974 **FIGURE 2** DNA binding by PlzA is c-di-GMP dependent. (**a**) EMSA with increasing
975 concentrations of $PlzA_{WT}$ showing binding to *glpFKD*(-219) DNA. The mixture was incubated
976 for 10 min before electrophoresis. (**b**) The same EMSA mixture as in (**a**) but with a final
977 concentration of 2.5 ng/μL of the nonspecific competitor poly-dI-dC. Protein was incubated
978 with poly-dI-dC for 5 min prior to the addition of labeled *glpFKD*(-219) probe. (**c**) The same
979 EMSA mixture as in (**b**) but supplemented with 100 μM c-di-GMP. Protein was incubated with
980 c-di-GMP for 5 min prior to the addition of any nucleic acids. Arrows indicate PlzA- *glpFKD*(-
981 219) complexes. Lane 1 in (**a-c**) is the probe only control, containing 50 nM of probe. Protein
982 concentrations are as follows in each subsequent lane: Lane 2: 0.5 μM, Lane 3: 1 μM, Lane

983 4: 2.5 μM, Lane 5: 5 μM, Lane 6: 7.5 μM, and Lane 7: 10 μM. (**d**), (**e**), (**f**) EMSA experiments
984 as in (**a**), (**b**), and (**c**), respectively, but performed with the mutant $PlzA_{RD-RD}$ protein. All
985 conditions were performed identically as with $PlzA_{WT}$. Each panel is a representative gel from
986 separate EMSAs which were performed in triplicate ($PlzA_{WT}$) or duplicate ($PlzA_{RD-RD}$).

987 **FIGURE 3** PlzA recognizes *glpFKD*(-219) and not pCR 2.1 sequences. (**a**) A schematic of the
988 unlabeled DNA competitors derived from the empty pCR 2.1 vector backbone or the vector
989 containing the *glpFKD*(-219) sequence. A labeled M13R and an unlabeled M13F primer were
990 used to amplify the target DNAs from the respective plasmids to generate competitors. These
991 competitors were then used as a control in competition EMSAs performed with labeled
992 *glpFKD*(-219) DNA probe. (**b**) Lane 1 and lane 2 are probe only and probe + $PlzA_{WT}$ controls
993 respectively. All lanes contained a c-di-GMP concentration of 100 μM, a final poly-dI-dC
994 concentration of 2.5 ng/μL, and a labeled *glpFKD*(-219) probe concentration of 50 nM. Lanes
995 2-8 contained a constant $PlzA_{WT}$ protein concentration of 1.5 μM. The unlabeled pCR 2.1
996 competitor was titrated into the reactions at increasing molar excess relative to labeled probe:
997 Lane 3-300 nM (6x), lane 4- 500 nM (10x), and lane 5- 1000 nM (20x). Unlabeled *glpFKD*(-
998 219) competitor was titrated into the reactions at increasing molar excess relative to labeled
999 probe: Lane 6- 300 nM (6x), lane 7- 500 nM (10x), and lane 8- 600 nM (12x). The free arrow
1000 indicates PlzA-*glpFKD*(-219) complexes. The pCR 2.1 competitor could not compete away the
1001 PlzA-*glpFKD*(-219) complex at any tested concentration. Unlabeled *glpFKD*(-219) competitor
1002 was able to compete at all tested concentrations as low as 6x molar excess.

1003 **FIGURE 4** Detection of c-di-GMP in recombinant $PlzA_{WT}$ and $PlzA_{RD-RD}$ by LC-MS/MS.
1004 Recombinant $PlzA_{WT}$ and $PlzA_{RD-RD}$ were sent off for mass spectrometry to detect c-di-GMP.
1005 Extracted ion chromatograms of the LC-MS/MS analysis for detection of c-di-GMP are
1006 displayed. Chromatograms depict the control c-di-GMP standard at 1 μM, recombinant
1007 $PlzA_{WT}$, and recombinant $PlzA_{RD-RD}$. The LC-MS/MS analysis reveals $PlzA_{WT}$ co-purified with
1008 c-di-GMP, but $PlzA_{RD-RD}$ did not. The concentration of c-di-GMP in recombinant $PlzA_{WT}$ was
1009 determined from a standard curve of c-di-GMP. $PlzA_{WT}$ co-purified with 99.29 nM of c-di-GMP

1010 and approximately 0.3% of the protein was bound with c-di-GMP. Black lines indicate
1011 chromatograms unrelated to this figure that were removed.

1012 **FIGURE 5** Levels of c-di-GMP alter DNA binding affinity of $PlzA_{WT}$. (**a**) A diagram of the
1013 generated DNA probe, designated as *glpFKD*(-7/+35), corresponding to a 42 bp sequence
1014 adjacent to the -10 site and proceeding 35 bp into the 5' UTR. An RNA probe was made
1015 corresponding to only nucleotides that are within the 5 'UTR which was designated as
1016 *glpFKD*(UTR) RNA. Probes were conjugated to a fluorescent molecule for the detection of
1017 binding in EMSAs. (**b**) EMSAs were performed with increasing protein concentrations of
1018 $PlzA_{WT,}$ and 10 nM fluorescently labeled probe at varying c-di-GMP concentrations (0,
1019 equimolar, 10, 25, 50, or 100 μM). For each EMSA shown, the indicated c-di-GMP
1020 concentration was held constant in all lanes. For each EMSA shown, lanes 1 and 7 are probe-
1021 only controls. Protein concentrations were as follows: Lane 2- 1 μM, Lane 3- 2.5 μM, Lane 4-
1022 3.5 μM, Lane 5- 5 μM, Lane 6- 7.5 μM. A final concentration of 2.5 ng/μL of the nonspecific
1023 competitor poly-dI-dC was added to each lane. Arrows indicate higher-order complexes
1024 formed as protein concentration increases. A representative gel for each tested c-di-GMP
1025 concentration is shown from triplicate EMSAs. (**c**) Triplicate EMSAs were quantitated by
1026 densitometry to determine the $K_{d(app)}$ of the $PlzA_{WT}$-*glpFKD*(-7/35+) interaction by nonlinear
1027 regression analysis using the one-site specific binding setting in GraphPad Prism. Errors bars
1028 represent one standard deviation (SD). (**d**) Bar graph displaying the calculated $K_{d(app)}$ ± the
1029 standard error of the mean (SEM). The $K_{d(app)}$ values from three EMSAs were analyzed by a
1030 Welch ANOVA with Dunnett's T3 multiple comparisons test via GraphPad Prism. Adjusted P-
1031 values are indicated as follows: ns= $p > 0.05$, *= $p \leq 0.05$, and ***= $p \leq 0.001$. Comparisons
1032 between 10, 25, 50, and 100 μM c-di-GMP are not indicated on the graph as they were not
1033 significant. (**e**) A similar EMSA experiment was performed as in Figure 5B but with $PlzA_{RD-RD}$
1034 and either 100 (lanes 1-6) or 0 (lanes 7-12) μM of c-di-GMP supplemented. No binding is
1035 observed.

1036 **FIGURE 6** $PlzA_{WT}$ also binds single stranded RNA and DNA. (**a**) Gradient EMSAs were
1037 performed with increasing protein concentrations of $PlzA_{WT}$ without c-di-GMP (left panel),
1038 equimolar (middle panel), or 100 μM c-di-GMP (right panel) and 10 nM fluorescently labeled
1039 *glpFKD*(UTR) RNA probe. Lane 1 is the probe-only control in each EMSA. Lane protein
1040 concentrations were as follows: Lane 2- 1 μM, Lane 3- 2.5 μM, Lane 4- 3.5 μM, Lane 5- 5 μM,
1041 Lane 6- 7.5 μM. (**b**) A similar EMSA experiment was performed with $PlzA_{RD\text{-}RD}$ with (lanes 1-
1042 8) or without (lanes 9-15) 100 μM c-di-GMP and 50 nM of *glpFKD*(UTR) RNA probe. Lane 1
1043 is a probe-only control. Protein concentrations were as follows: Lanes 2 and 9- 1 μM, Lanes
1044 3 and 10- 1.25 μM, Lanes 4 and 11- 2 μM, Lanes 5 and 12- 2.5 μM, Lanes 6 and 13- 3.3 μM,
1045 Lanes 7 and 14- 5 μM, Lanes 8 and 15- 10 μM. Riboguard was supplemented in the $PlzA_{RD\text{-}}$
1046 $_{RD}$ EMSA mixtures to a final concentration of 4 U/μL. (**c**) Gradient EMSAs were performed with
1047 increasing protein concentrations of $PlzA_{WT}$ with 100 μM c-di-GMP (left panel) or 0 μM c-di-
1048 GMP (right panel) with 10 nM fluorescently labeled ss*glpF* probe. Lanes 1 and 7 are the probe-
1049 only control in each EMSA. Lane protein concentrations were as follows: Lanes 2 and 8- 1
1050 μM, Lanes 3 and 9- 2.5 μM, Lanes 4 and 10- 3.5 μM, Lanes 5 and 11- 5 μM, Lanes 6 and 12-
1051 7.5 μM. Representative gels are shown from triplicate ($PlzA_{WT}$) or duplicate ($PlzA_{RD\text{-}RD}$) EMSA
1052 experiments. (**d**) Triplicate EMSAs from (**a**) and (**c**) were quantitated by densitometry to
1053 determine the $K_{d(app)}$ of $PlzA_{WT}$ for the *glpFKD* RNA or ssDNA interactions by nonlinear
1054 regression analysis using the one-site specific binding setting in GraphPad Prism. Errors bars
1055 represent one standard deviation (SD).

1056 **FIGURE 7** c-di-GMP significantly impacts PlzA-nucleic acid binding and PlzA prefers dsDNA
1057 and RNA over ssDNA. (**a**) The $K_{d(app)}$ values from triplicate RNA EMSAs at each tested c-di-
1058 GMP concentration in Figure 6A were analyzed by a Welch ANOVA with Dunnett's T3 multiple
1059 comparisons test. (**b**) The $K_{d(app)}$ values from triplicate ssDNA EMSAs at the tested c-di-GMP
1060 concentrations in Figure 6C were analyzed by a Welch's t-test. (**c**) The $K_{d(app)}$ values from
1061 EMSAs with PlzA and each tested nucleic acid at 100 μM c-di-GMP were compared via a
1062 Welch ANOVA with Dunnett's T3 multiple comparisons test. Bar graphs display the calculated

1063 $K_{d(app)s}$ ± the standard error of the mean (SEM). Adjusted P-values are indicated as follows:
1064 ns= p >0.05, *= p ≤0.05, and **= p ≤0.01.

1065 **FIGURE 8** The N-terminal domain of PlzA is the nucleic acid binding domain. (**a**) The cloning
1066 strategy used to produce recombinant N ($PlzA_{NTD}$) and C ($PlzA_{CTD}$) terminal PlzA domains.
1067 The *plzA* gene portions corresponding to the N-terminus, *plzA*-NTD, and the C-terminus, *plzA*-
1068 CTD, were generated and cloned into an expression vector to produce recombinant $PlzA_{NTD}$
1069 and $PlzA_{CTD}$ proteins. Gradient EMSAs were performed with increasing protein concentrations
1070 of $PlzA_{NTD}$ (**b, d**) or $PlzA_{CTD}$ (**c, e**) with (lanes 1-6) or without (lanes 7-12) 100 μM c-di-GMP
1071 and 10 nM fluorescently labeled *glpFKD*(-7/35+) dsDNA (**b, c**) or *glpFKD*(UTR) RNA (**d, e**)
1072 probe. Lanes 1 and 7 are probe-only controls. Protein concentrations were as follows: Lanes
1073 2 and 8- 0.5 μM, Lanes 3 and 9- 1 μM, Lanes 4 and 10- 2.5 μM, Lanes 5 and 11- 5 μM, Lanes
1074 6 and 12- 7.5 μM. SUPERase•In RNase inhibitor was supplemented to a final concentration
1075 of 2 U/μL in RNA EMSA mixtures. The asterisk indicates $PlzA_{NTD}$-dsDNA shifts.
1076 Representative gels are shown from triplicate ($PlzA_{NTD}$) or duplicate ($PlzA_{CTD}$) EMSAs. N= 2
1077 or 3 independent experiments.

1078 **FIGURE 9** Detection of c-di-GMP in recombinant $PlzA_{NTD}$ and $PlzA_{CTD}$ by LC-MS/MS and
1079 circular dichroism of proteins. (**a**) Recombinant $PlzA_{NTD}$ and $PlzA_{CTD}$ were sent off for mass
1080 spectrometry to detect the presence of c-di-GMP. Extracted ion chromatograms of the LC-
1081 MS/MS analysis are displayed. Chromatograms depict the control c-di-GMP standard at 1 μM,
1082 recombinant $PlzA_{CTD}$, and recombinant $PlzA_{NTD}$. The LC-MS/MS analysis revealed that
1083 $PlzA_{CTD}$ co-purified with c-di-GMP, but $PlzA_{NTD}$ did not. The concentration of c-di-GMP in
1084 recombinant $PlzA_{CTD}$ was determined from a standard curve of c-di-GMP. $PlzA_{CTD}$ co-purified
1085 with 704.29 nM of c-di-GMP and approximately 1.1 % of the protein was bound with c-di-GMP.
1086 The c-di-GMP standard chromatogram shown is the same as in Figure 4. (**b**) Circular
1087 dichroism spectra of recombinant $PlzA_{WT}$, $PlzA_{RD-RD}$, $PlzA_{NTD}$, and $PlzA_{CTD}$ measured in EMSA
1088 buffer (see methods). EMSA buffer alone or plus 50 μM c-di-GMP were also measured as
1089 controls.

1090 **FIGURE 10** Computational docking analysis of PlzA with *glp* DNA and RNA. Computational
1091 docking was performed using the HDOCK server with PlzA and either (**a**) the 42 bp *glpFKD*(-
1092 7/+35) dsDNA or (**b**) the *glpFKD*(UTR) RNA sequence. In (**a**) only 26 of 42 bp of the *glpFKD*(-
1093 7/+35) sequence is shown. The dashed lines represent where bases were left out of the figure
1094 to zoom in on the protein-DNA interactions. The dsDNA model was linear, and removal of the
1095 bases has no impact on the interpretation of the data. The top predicted model from each
1096 computation is shown. The HDOCK docking and confidence scores for each model were -
1097 210.60 and 0.77 for PlzA-*glp* DNA, and -280.71 and 0.93 for PlzA-*glp* RNA, respectively. The
1098 protein is rotated 180° from the top to the bottom panels. Select amino acid residues that
1099 interface the nucleic acids are labeled.

1100 **FIGURE 11** Model depicting the modulation of PlzA function by levels of c-di-GMP. Apo and
1101 holo-PlzA are hypothesized to have distinct functions in the vertebrate and tick hosts
1102 respectively. Recent studies identified PlzA RNA chaperone activity that is c-di-GMP
1103 independent (Van Gundy *et al.*, 2023). In environments with no c-di-GMP, such as the
1104 vertebrate host, apo-PlzA engages in RNA chaperone activity to modulate gene expression
1105 required for survival in the vertebrate host. The phosphodiesterases PdeA and PdeB are likely
1106 to be highly active upon transmission and into vertebrate infection, lowering c-di-GMP levels
1107 and facilitating apo-PlzA functions (Sultan *et al.*, 2010; Pitzer *et al.*, 2011; Sultan *et al.*, 2011;
1108 Novak *et al.*, 2014; Groshong *et al.*, 2021). Phosphodiesterase activity is likely to occur at all
1109 stages to regulate c-di-GMP levels and indirectly, PlzA function. When Hk1 is activated (signal
1110 unknown), Rrp1 is phosphorylated and produces c-di-GMP. Holo-PlzA can also engage in
1111 RNA chaperone activity by annealing RNAs, and potentially interact with RNAP (Grassmann
1112 *et al.*, 2023; Van Gundy *et al.*, 2023). We propose that levels of c-di-GMP impact the specific
1113 genes regulated by PlzA through altering nucleic acid binding affinity. At lower c-di-GMP
1114 levels, few holo-PlzA monomers exist resulting in weak PlzA binding affinity for certain target
1115 genes such as *glpFKD*. As levels of c-di-GMP increase, such as in the tick host or during a
1116 blood meal, more holo-PlzA molecules bind target genes with higher affinity, and PlzA could

1117 potentially multimerize on DNA. At high protein and c-di-GMP concentrations, we hypothesize

1118 release of DNA by holo-PlzA via a yet unknown signal.

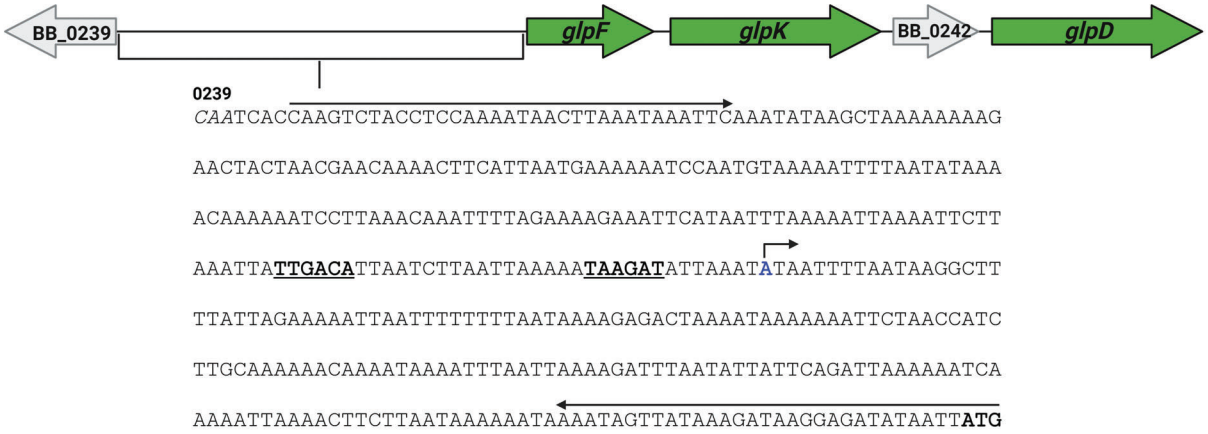


**FIGURE 1** The *glpFKD* operon, 5' UTR, and designed probe schematic. The glycerol catabolism gene operon (*glpFKD*) contains four genes: *glpF* (BB_0240, glycerol uptake facilitator protein), *glpK* (BB_0241, glycerol kinase), BB_0242 (hypothetical protein), and *glpD* (BB_0243, glycerol-3-phosphate dehydrogenase). The promoter and transcriptional boundaries were previously mapped (Grove et al., 2017). The -35 and -10 sites are bolded and underlined. The transcriptional start site nucleotide is highlighted in blue and topped with an arrow indicating the direction of transcription. The start of the *glpF* ORF is marked by the bolded ATG, while the start of the upstream BB_0239 ORF is labeled, and its nucleotides are italicized. The long arrows indicate the location of primers used to generate a large probe incorporating the entire intergenic region which is denoted as *glpFKD*(-219) for initial DNA binding studies.

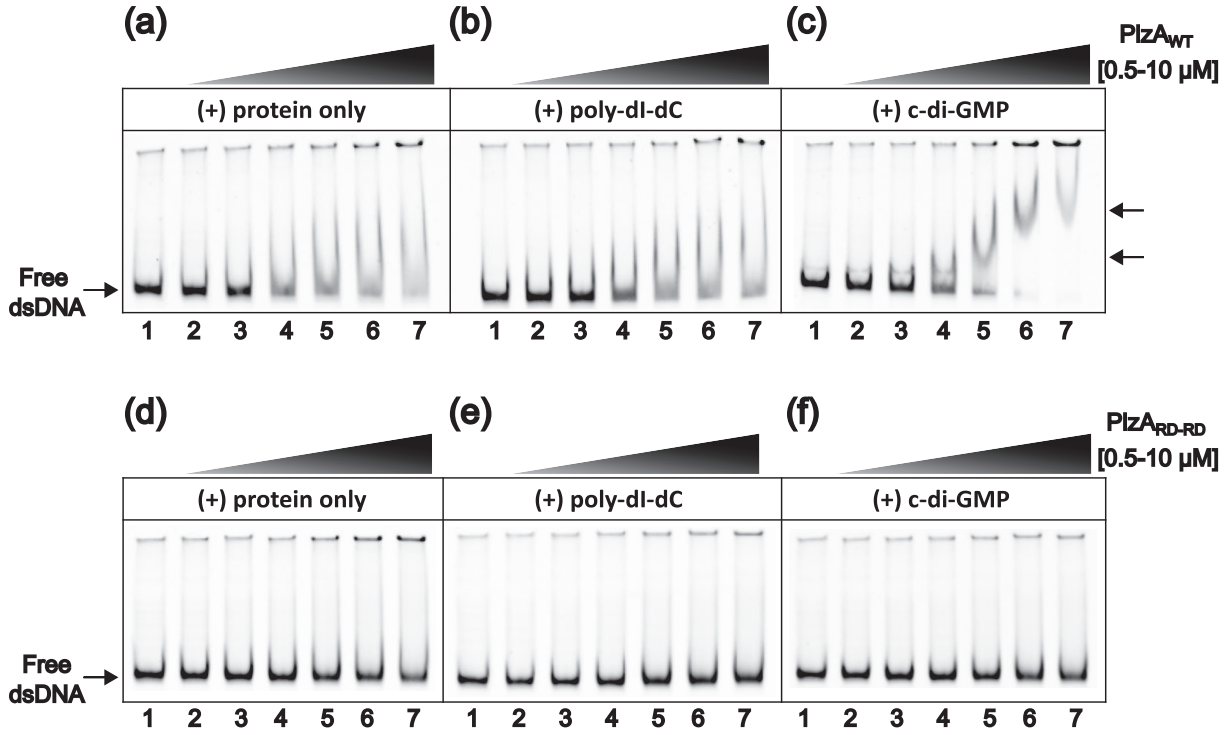


**FIGURE 2** DNA binding by PlzA is c-di-GMP dependent. (**a**) EMSA with increasing concentrations of PlzA$_{WT}$ showing binding to *glpFKD*(-219) DNA. The mixture was incubated for 10 min before electrophoresis. (**b**) The same EMSA mixture as in (a) but with a final concentration of 2.5 ng/μL of the nonspecific competitor poly-dI-dC. Protein was incubated with poly-dI-dC for 5 min prior to the addition of labeled *glpFKD*(-219) probe. (**c**) The same EMSA mixture as in (**b**) but supplemented with 100 μM c-di-GMP. Protein was incubated with c-di-GMP for 5 min prior to the addition of any nucleic acids. Arrows indicate PlzA- *glpFKD*(-219) complexes. Lane 1 in (**a**-**c**) is the probe only control, containing 50 nM of probe. Protein concentrations are as follows in each subsequent lane: Lane 2: 0.5 μM, Lane 3: 1 μM, Lane 4: 2.5 μM, Lane 5: 5 μM, Lane 6: 7.5 μM, and Lane 7: 10 μM. (**d**), (**e**), (**f**) EMSA experiments as in (**a**), (**b**), and (**c**), respectively, but performed with the mutant PlzA$_{RD-RD}$ protein. All conditions were performed identically as with PlzA$_{WT}$. Each panel is a representative gel from separate EMSAs which were performed in triplicate (PlzA$_{WT}$) or duplicate (PlzA$_{RD-RD}$).

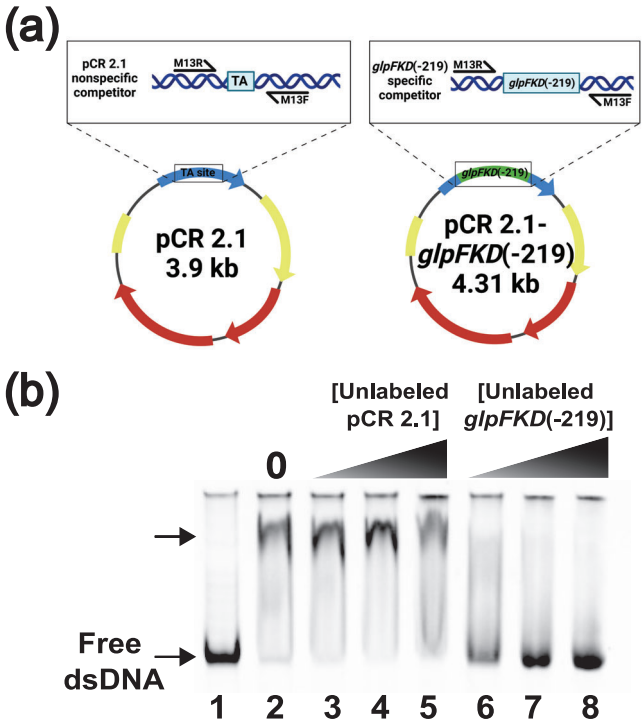


**FIGURE 3** PlzA recognizes *glpFKD*(-219) and not pCR 2.1 sequences. (**a**) A schematic of the unlabeled DNA competitors derived from the empty pCR 2.1 vector backbone or the vector containing the *glpFKD*(-219) sequence. A labeled M13R and an unlabeled M13F primer were used to amplify the target DNAs from the respective plasmids to generate competitors. These competitors were then used as a control in competition EMSAs performed with labeled *glpFKD*(-219) DNA probe. (**b**) Lane 1 and lane 2 are probe only and probe + $PlzA_{WT}$ controls respectively. All lanes contained a c-di-GMP concentration of 100 μM, a final poly-dI-dC concentration of 2.5 ng/μL, and a labeled *glpFKD*(-219) probe concentration of 50 nM. Lanes 2-8 contained a constant $PlzA_{WT}$ protein concentration of 1.5 μM. The unlabeled pCR 2.1 competitor was titrated into the reactions at increasing molar excess relative to labeled probe: Lane 3-300 nM (6x), lane 4- 500 nM (10x), and lane 5- 1000 nM (20x). Unlabeled *glpFKD(*-219) competitor was titrated into the reactions at increasing molar excess relative to labeled probe: Lane 6-300 nM (6x), lane 7- 500 nM (10x), and lane 8- 600 nM (12x). The free arrow indicates PlzA-*glpFKD*(-219) complexes. The pCR 2.1 competitor could not compete away the PlzA-*glpFKD*(-219) complex at any tested concentration. Unlabeled *glpFKD*(-219) competitor was able to compete at all tested concentrations as low as 6x molar excess.

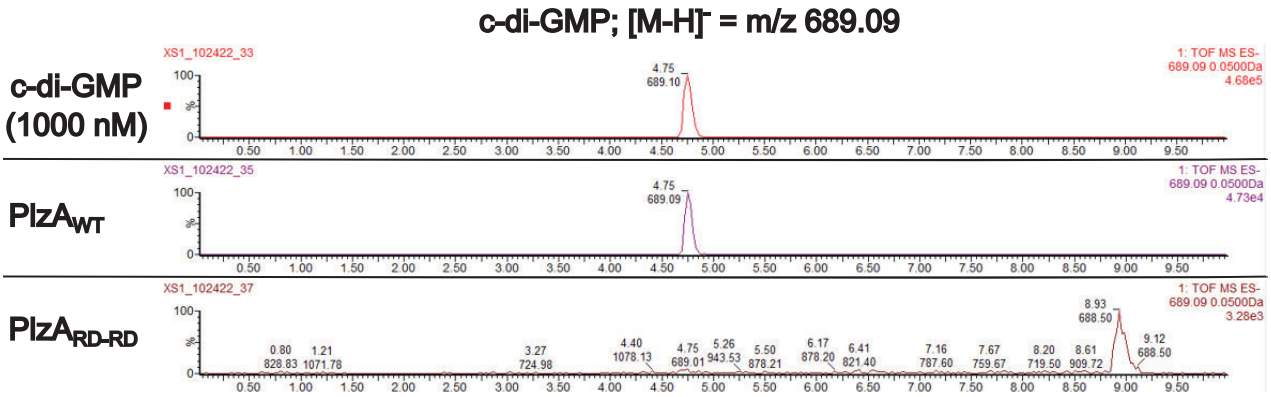


**FIGURE 4** Detection of c-di-GMP in recombinant PlzA$_{WT}$ and PlzA$_{RD-RD}$ by LC-MS/MS. Recombinant PlzA$_{WT}$ and PlzA$_{RD-RD}$ were sent off for mass spectrometry to detect c-di-GMP. Extracted ion chromatograms of the LC-MS/MS analysis for detection of c-di-GMP are displayed. Chromatograms depict the control c-di-GMP standard at 1 μM, recombinant PlzA$_{WT}$, and recombinant PlzA$_{RD-RD}$. The LC-MS/MS analysis reveals PlzA$_{WT}$ co-purified with c-di-GMP, but PlzA$_{RD-RD}$ did not. The concentration of c-di-GMP in recombinant PlzA$_{WT}$ was determined from a standard curve of c-di-GMP. PlzA$_{WT}$ co-purified with 99.29 nM of c-di-GMP and approximately 0.3% of the protein was bound with c-di-GMP. Black lines indicate chromatograms unrelated to this figure that were removed.

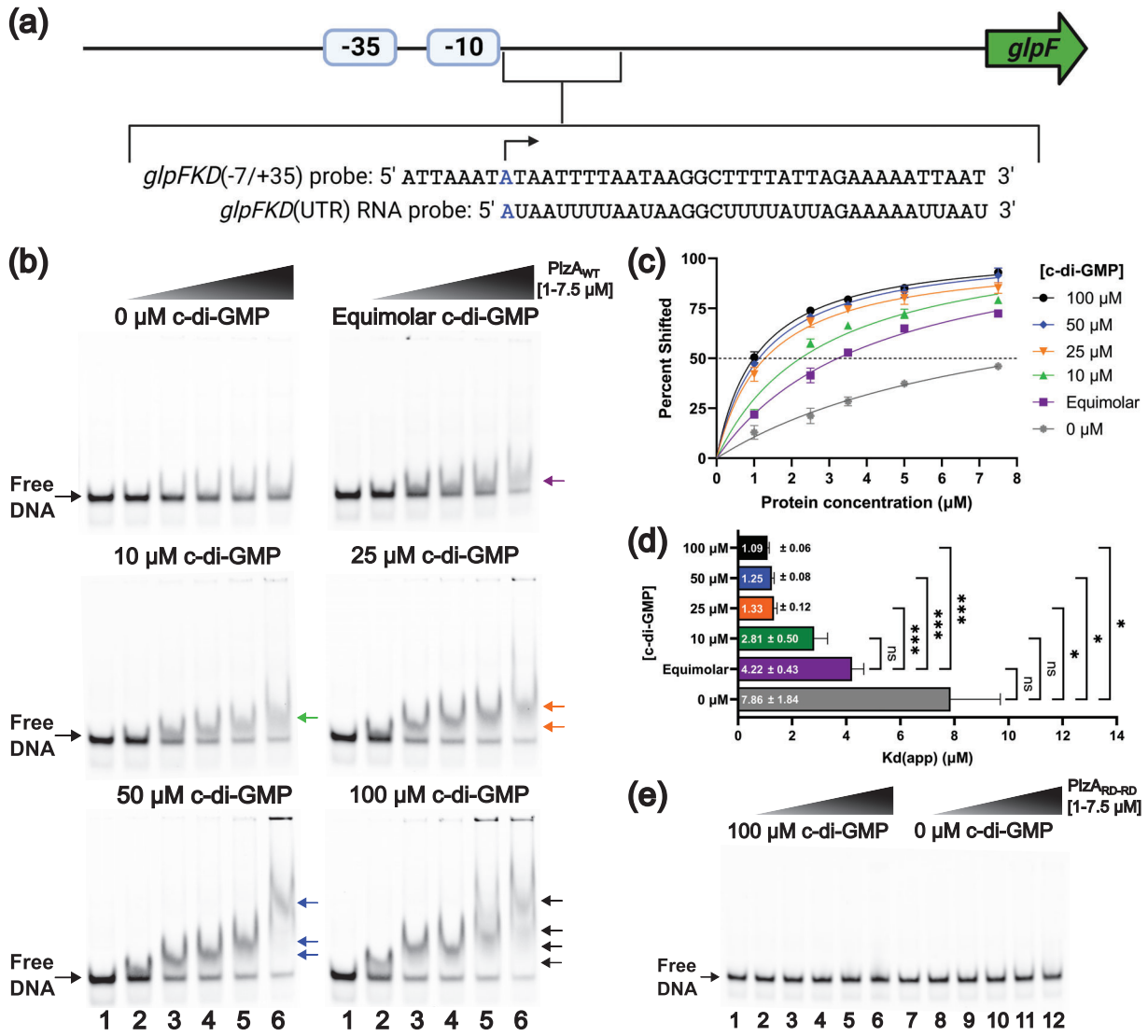


**FIGURE 5** Levels of c-di-GMP alter DNA binding affinity of $PlzA_{WT}$. (a) A diagram of the generated DNA probe, designated as *glpFKD(*-7/+35), corresponding to a 42 bp sequence adjacent to the -10 site and proceeding 35 bp into the 5' UTR. An RNA probe was made corresponding to only nucleotides that are within the 5 'UTR which was designated as *glpFKD*(UTR) RNA. Probes were conjugated to a fluorescent molecule for the detection of binding in EMSAs. (b) EMSAs were performed with increasing protein concentrations of $PlzA_{WT}$, and 10 nM fluorescently labeled probe at varying c-di-GMP concentrations (0, equimolar, 10, 25, 50, or 100 μM). For each EMSA shown, the indicated c-di-GMP concentration was held constant in all lanes. For each EMSA shown, lanes 1 and 7 are probe-only controls. Protein concentrations were as follows: Lane 2- 1 μM, Lane 3- 2.5 μM, Lane 4- 3.5 μM, Lane 5- 5 μM, Lane 6- 7.5 μM. A final concentration of 2.5 ng/μL of the nonspecific competitor poly-dI-dC was added to each lane. Arrows indicate higher-order complexes formed as protein concentration increases. A representative gel for each tested c-di-GMP concentration is shown from triplicated EMSAs. (c) Triplicate EMSAs were quantitated by densitometry to determine the $K_{d(app)}$ of the $PlzA_{WT}$-*glpFKD*(-7/35+) interaction by nonlinear regression analysis using the one-site specific binding setting in GraphPad Prism. Errors bars represent one standard deviation (SD). (d) Bar graph displaying the calculated $K_{d(app)}$ ± the standard error of the mean (SEM). The Kd(app) values from three EMSAs were analyzed by a Welch ANOVA with Dunnett's T3 multiple comparisons test via GraphPad Prism. Adjusted P-values are indicated as follows: ns= p >0.05, *= p ≤0.05, and ***= p ≤0.001. Comparisons between 10, 25, 50, and 100 μM c-di-GMP are not indicated on the graph as they were not significant. (e) A similar EMSA experiment was performed as in Figure 5B but with $PlzA_{RD-RD}$ and either 100 (lanes 1-6) or 0 (lanes 7-12) μM of c-di-GMP supplemented. No binding is observed.

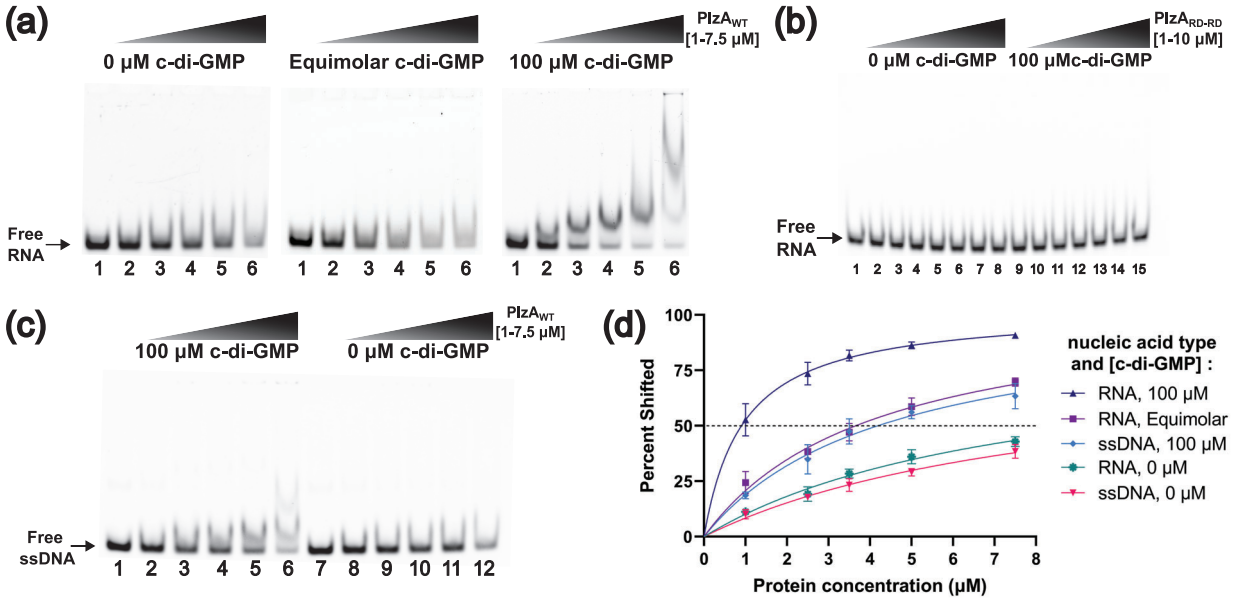


**FIGURE 6** PlzA$_{WT}$ also binds single stranded RNA and DNA. (**a**) Gradient EMSAs were performed with increasing protein concentrations of PlzA$_{WT}$ without c-di-GMP (left panel), equimolar (middle panel), or 100 μM c-di-GMP (right panel) and 10 nM fluorescently labeled *glpFKD*(UTR) RNA probe. Lane 1 is the probe-only control in each EMSA. Lane protein concentrations were as follows: Lane 2- 1 μM, Lane 3- 2.5 μM, Lane 4- 3.5 μM, Lane 5- 5 μM, Lane 6- 7.5 μM. (**b**) A similar EMSA experiment was performed with PlzA$_{RD-RD}$ with (lanes 1-8) or without (lanes 9-15) 100 μM c-di-GMP and 50 nM of *glpFKD*(UTR) RNA probe. Lane 1 is a probe-only control. Protein concentrations were as follows: Lanes 2 and 9- 1 μM, Lanes 3 and 10- 1.25 μM, Lanes 4 and 11- 2 μM, Lanes 5 and 12- 2.5 μM, Lanes 6 and 13- 3.3 μM, Lanes 7 and 14- 5 μM, Lanes 8 and 15- 10 μM. Riboguard was supplemented in the PlzA$_{RD-RD}$ EMSA mixtures to a final concentration of 4 U/μL. (**c**) Gradient EMSAs were performed with increasing protein concentrations of PlzA$_{WT}$ with 100 μM c-di-GMP (left panel) or 0 μM c-di-GMP (right panel) with 10 nM fluorescently labeled ss*glpF* probe. Lanes 1 and 7 are the probe-only control in each EMSA. Lane protein concentrations were as follows: Lanes 2 and 8- 1 μM, Lanes 3 and 9- 2.5 μM, Lanes 4 and 10- 3.5 μM, Lanes 5 and 11- 5 μM, Lanes 6 and 12- 7.5 μM. Representative gels are shown from triplicated (PlzA$_{WT}$) or duplicated (PlzA$_{RD-RD)}$ EMSA experiments. (**d**) Triplicated EMSAs from (**a**) and (**c**) were quantitated by densitometry to determine the Kd(app) of PlzA$_{WT}$ for the *glpFKD* RNA or ssDNA interactions by nonlinear regression analysis using the one-site specific binding setting in GraphPad Prism. Errors bars represent one standard deviation (SD).

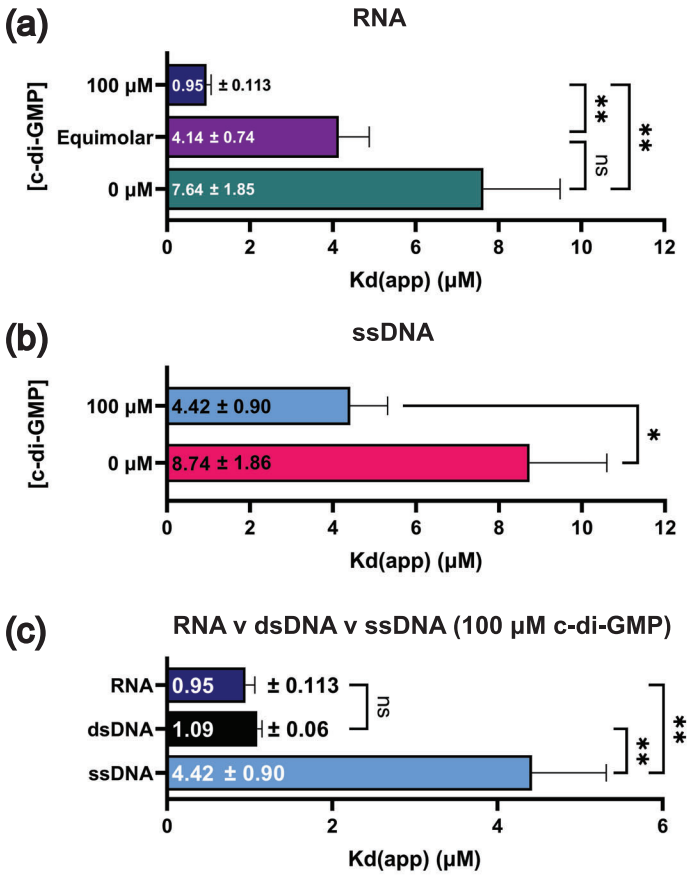


**FIGURE 7** c-di-GMP significantly impacts PlzA-nucleic acid binding and PlzA prefers dsDNA and RNA over ssDNA. (**a**) The Kd(app) values from triplicate RNA EMSAs at each tested c-di-GMP concentration in Figure 6A were analyzed by a Welch ANOVA with Dunnett's T3 multiple comparisons test. (**b**) The Kd(app) values from triplicate ssDNA EMSAs at the tested c-di-GMP concentrations in Figure 6C were analyzed by a Welch's t-test. (c) The Kd(app) values from EMSAs with PlzA and each tested nucleic acid at 100 μM c-di-GMP were compared via a Welch ANOVA with Dunnett's T3 multiple comparisons test. Bar graphs display the calculated Kd(app)s ± the standard error of the mean (SEM). Adjusted P-values are indicated as follows: ns= p >0.05, *= p ≤0.05, and **= p ≤0.01.

**Table 1.** Binding interaction summary of $PlzA_{WT}$ and the tested nucleic acids at various c-di-GMP concentrations.

| ***glpFKD*(-7/+35) dsDNA** | | | |
|---|---|---|---|
| **c-di-GMP (μM)** | **$K_{d(app)}$ (μM), 95% C.I. [LL, UL]** | **$B_{max}$ (% Shifted), 95% C.I. [LL, UL]** | **Adj. R-squared** |
| 100 | 1.09, [0.97, 1.23] | 105.20, [102.20, 108.40] | 0.986 |
| 50 | 1.25, [1.08, 1.45] | 105.50, [101.50, 109.90] | 0.981 |
| 25 | 1.33, [1.10, 1.59] | 101.60, [96.58, 107.10] | 0.971 |
| 10 | 2.81, [1.98, 4.02] | 113.00, [98.79, 132.30] | 0.940 |
| Equimolar | 4.22, [3.40, 5.26] | 115.40, [104.40, 129.10] | 0.983 |
| 0 | 7.86, [4.85, 14.06] | 94.25, [71.72, 138.80] | 0.950 |
| ***glpFKD*(UTR) RNA** | | | |
| **c-di-GMP (μM)** | **$K_{d(app)}$ (μM), 95% C.I. [LL, UL]** | **$B_{max}$ (% Shifted), 95% C.I. [LL, UL]** | **Adj. R-squared** |
| 100 | 0.95, [0.73, 1.22] | 102.6, [96.76, 109.20] | 0.930 |
| Equimolar | 4.14, [2.79, 6.30] | 106.7, [89.50, 132.60] | 0.944 |
| 0 | 7.64, [4.71, 13.66] | 87.73, [66.88, 128.80] | 0.950 |
| ***glpF* ssDNA** | | | |
| **c-di-GMP (μM)** | **$K_{d(app)}$ (μM), 95% C.I. [LL, UL]** | **Bmax (% Shifted), 95% C.I. [LL, UL]** | **Adj. R-squared** |
| 100 | 4.42, [2.94, 6.84] | 102.80, [85.32, 129.90] | 0.920 |
| 0 | 8.74, [5.67, 14.70] | 82.04, [63.53, 116.90] | 0.950 |

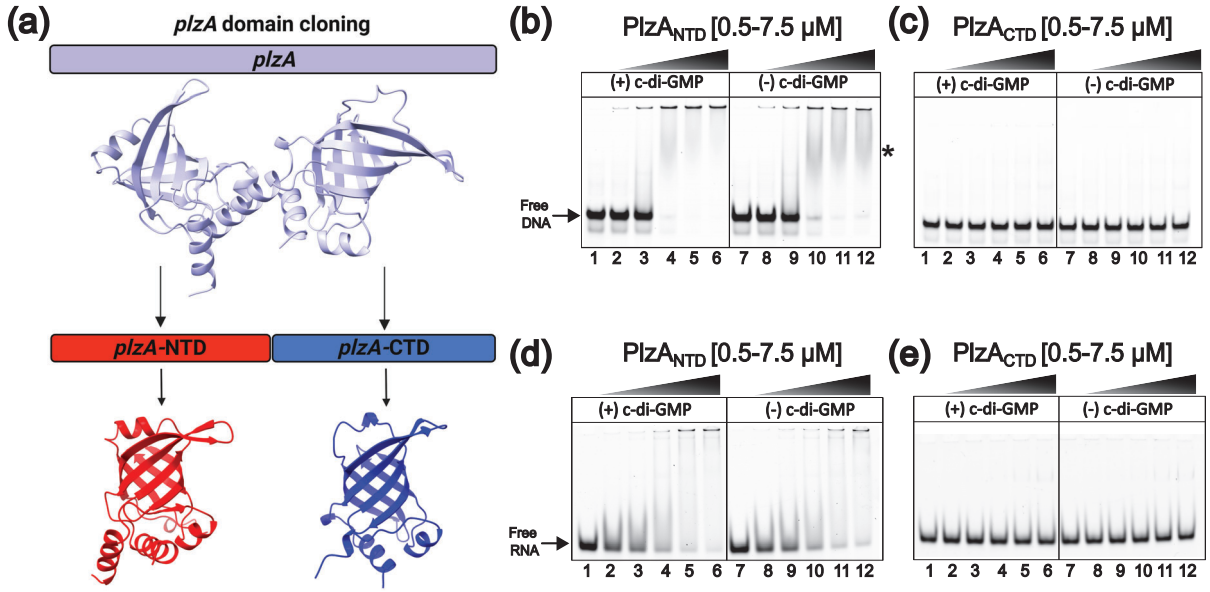


**FIGURE 8** The N-terminal domain of PlzA is the nucleic acid binding domain. (**a**) The cloning strategy used to produce recombinant N (PlzA$_{NTD}$) and C (PlzA$_{CTD}$) terminal PlzA domains. The plzA gene portions corresponding to the N-terminus, plzA-NTD, and the C-terminus, plzA-CTD, were generated and cloned into an expression vector to produce recombinant PlzA$_{NTD}$ and PlzA$_{CTD}$ proteins. Gradient EMSAs were performed with increasing protein concentrations of PlzA$_{NTD}$ (**b**, **d**) or PlzA$_{CTD}$ (**c**, **e**) with (lanes 1-6) or without (lanes 7-12) 100 μM c-di-GMP and 10 nM fluorescently labeled *glpFKD*(-7/35+) dsDNA (b, c) or *glpFKD*(UTR) RNA (**d**, **e**) probe. Lanes 1 and 7 are probe-only controls. Protein concentrations were as follows: Lanes 2 and 8- 0.5 μM, Lanes 3 and 9- 1 μM, Lanes 4 and 10- 2.5 μM, Lanes 5 and 11- 5 μM, Lanes 6 and 12- 7.5 μM. SUPERase•In RNase inhibitor was supplemented to a final concentration of 2 U/μL in RNA EMSA mixtures. Representative gels are shown from triplicated (PlzA$_{NTD}$) or duplicated (PlzA$_{CTD}$) EMSAs.

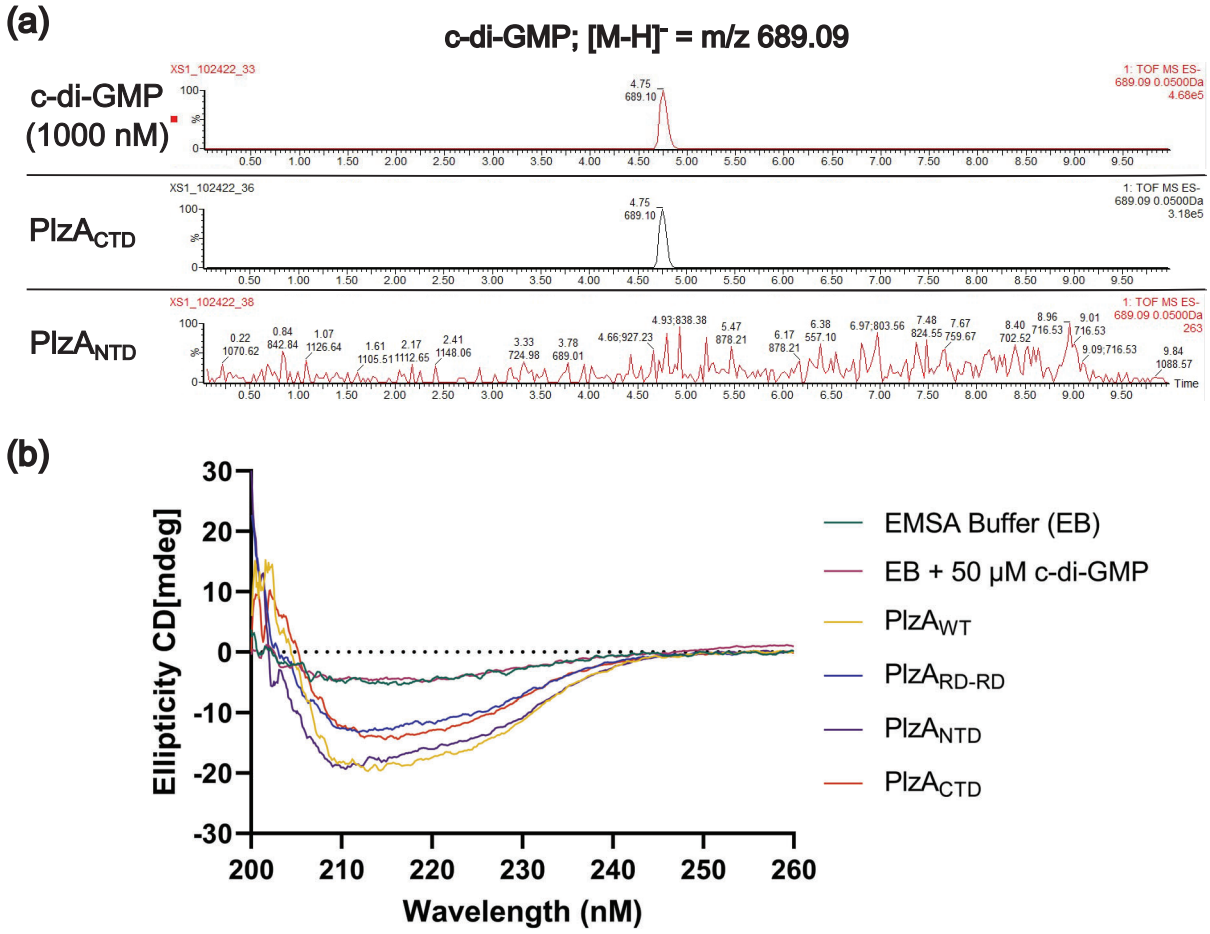


**FIGURE 9** Detection of c-di-GMP in recombinant $PlzA_{NTD}$ and $PlzA_{CTD}$ by LC-MS/MS and circular dichroism of proteins. (**a**) Recombinant $PlzA_{NTD}$ and $PlzA_{CTD}$ were sent off for mass spectrometry to detect the presence of c-di-GMP. Extracted ion chromatograms of the LC-MS/MS analysis are displayed. Chromatograms depict the control c-di-GMP standard at 1 μM, recombinant $PlzA_{CTD}$, and recombinant $PlzA_{NTD}$. The LC-MS/MS analysis revealed that $PlzA_{CTD}$ co-purified with c-di-GMP, but $PlzA_{NTD}$ did not. The concentration of c-di-GMP in recombinant $PlzA_{CTD}$ was determined from a standard curve of c-di-GMP. $PlzA_{CTD}$ co-purified with 704.29 nM of c-di-GMP and approximately 1.1 % of the protein was bound with c-di-GMP. The c-di-GMP standard chromatogram shown is the same as in Figure 4. (**b**) Circular dichroism spectra of recombinant $PlzA_{WT}$, $PlzA_{RD-RD}$, $PlzA_{NTD}$, and $PlzA_{CTD}$ measured in EMSA buffer (see methods). EMSA buffer alone or plus 50 μM c-di-GMP were also measured as controls.

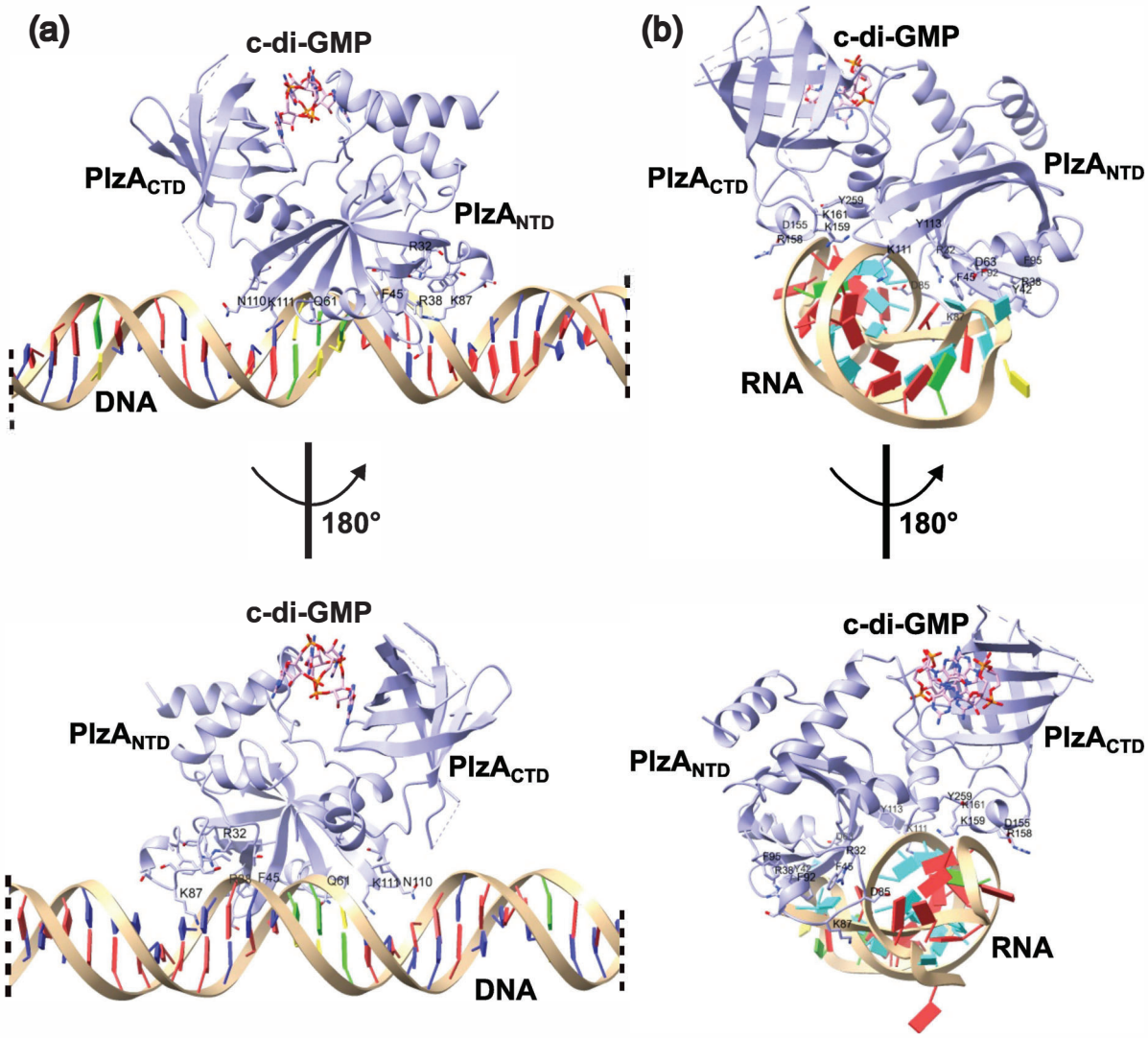


**FIGURE 10** Computational docking analysis of PlzA with *glp* DNA and RNA. Computational docking was performed using the HDOCK server with PlzA and either (a) the 42 bp *glpFKD*(-7/+35) dsDNA or (b) the *glpFKD*(UTR) RNA sequence. In (a) only 26 of 42 bp of the *glpFKD*(-7/+35) sequence is shown. The dashed lines represent where bases were left out of the figure to zoom in on the protein-DNA interactions. The dsDNA model was linear, and removal of the bases has no impact on the interpretation of the data. The top predicted model from each computation is shown. The HDOCK docking and confidence scores for each model were -210.60 and 0.77 for PlzA-*glp* DNA and -280.71 and 0.93 for PlzA-*glp* RNA, respectively. The protein is rotated 180° from the top to the bottom panels. Select amino acid residues that interface the nucleic acids are labeled.

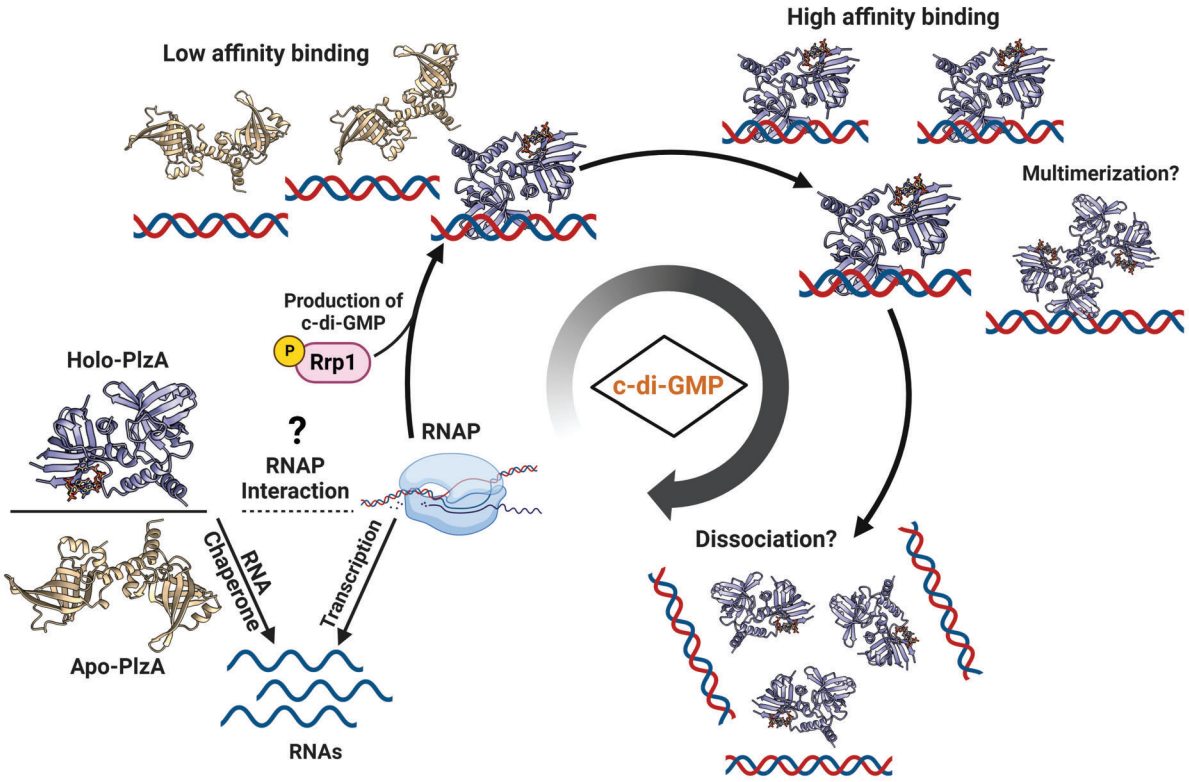


**FIGURE 11** Model depicting the modulation of PlzA function by levels of c-di-GMP. Apo and holo-PlzA are hypothesized to have distinct functions in the vertebrate and tick hosts respectively. Recent studies identified PlzA RNA chaperone activity that is c-di-GMP independent (Van Gundy et al., 2023). In environments with no c-di-GMP, such as the vertebrate host, apo-PlzA engages in RNA chaperone activity to modulate gene expression required for survival in the vertebrate host. The phosphodiesterases PdeA and PdeB are likely to be highly active upon transmission and into vertebrate infection, lowering c-di-GMP levels and facilitating apo-PlzA functions (Sultan et al., 2010; Pitzer et al., 2011; Sultan et al., 2011; Novak et al., 2014; Groshong et al., 2021). Phosphodiesterase activity is likely to occur at all stages to regulate c-di-GMP levels and indirectly, PlzA function. When Hk1 is activated (signal unknown), Rrp1 is phosphorylated and produces c-di-GMP. Holo-PlzA can also engage in RNA chaperone activity by annealing RNAs, and potentially interact with RNAP (Grassmann et al., 2023; Van Gundy et al., 2023). We propose that levels of c-di-GMP impact the specific genes regulated by PlzA through altering nucleic acid binding affinity. At lower c-di-GMP levels, few holo-PlzA monomers exist resulting in weak PlzA binding affinity for certain target genes such as *glpFKD*. As levels of c-di-GMP increase, such as in the tick host or during a blood meal, more holo-PlzA molecules bind target genes with higher affinity, and PlzA could potentially multimerize on DNA. At high protein and c-di-GMP concentrations, we hypothesize release of DNA by holo-PlzA via a yet unknown signal.

**Table 2.** Oligonucleotides used in this study.

| Target | Name and Sequence (5' → 3') | Size (bp) |
|---|---|---|
| **Cloning and Sequencing Primers** | | |
| *plzA* | *plzA* F:<br>GGCAGC**CATATG**CTTTTATCTAGAAAAATAAGAGATTATG<br>*plzA* R:<br>GTGGTG**CTCGAG**TTAATTGAAATAATCATGGATCAAC | 786 |
| MCS pET28a(+):*plzA* | T7 F:<br>TAATACGACTCACTATAGGG<br>T7 R:<br>TAGTTATTGCTCAGCGGTGG | 1026 |
| pCR 2.1 TA clones | M13 F:<br>GTAAAACGACGGCCAG<br>M13 R:<br>CAGGAAACAGCTATGAC | N/A |
| *plzA*-NTD | *plzA* 1F:<br>ATGCTTTTATCTAGAAAAATAAGAGATTATG<br>plzA N R:<br>TTACTGATTTTGCCCAAGCTTTAAATC | 435 |
| *plzA*-CTD | *plzA* C F:<br>ATGGATTTAAAGCTTGGGCAA<br>plzA 1R:<br>ATTGAAATAATCATGGATCAACATAGTATAC | 378 |
| **Site-directed Mutagenesis Primers** | | |
| *plzA* R145-149D | *plzA*-mut F:<br>AATCAGGACATTCATGAGGACATTATTATCGATAAAGATTCTATTAG<br>plzA-mut R:<br>GTCCTCATGAATGTCCTGATTTTGCCCAAGCTTTAAATCAAGAAGCTTTCC | 786 |
| **EMSA Probes, Competitors, and Primers** | | |
| *glpFKD*(-219) | M13 F:<br>GTAAAACGACGGCCAG<br>M13 R 5'IRD800CW or unlabeled:<br>CAGGAAACAGCTATGAC | 654 |
| *glpFKD*(-7/+35) | *glpF* F IRD800:<br>ATTAAATATAATTTTAATAAGGCTTTTATTAGAAAAATTAAT<br>*glpF* R:<br>ATTAATTTTTCTAATAAAAGCCTTATTAAAATTATATTTAAT | 42 |
| ss*glpF* | *glpF* F IRD800:<br>ATTAAATATAATTTTAATAAGGCTTTTATTAGAAAAATTAAT | 42 |
| *glpFKD*(UTR) RNA | *glpF* RNA 5' Alexa488:<br>AUAAUUUUAAUAAGGCUUUUAUUAGAAAAAUUAAU | 35 |
| pCR 2.1 competitor | M13 F:<br>GTAAAACGACGGCCAG<br>M13 R:<br>CAGGAAACAGCTATGAC | 210 |

[a] Bolded and underlined nucleotides indicate restriction enzyme sites.